communications earth & environment

Article

A Nature Portfolio journal

https://doi.org/10.1038/s43247-025-03031-4

Environmentally adjusted $\delta^{13}C$ thresholds for accurate detection of C_4 plant consumption in Europe

Margaux L. C. Depaermentier [1,3] ✉, Michael Kempf [2,3] ✉ & Giedrė Motuzaitė Matuzevičiūtė [1]

Detecting C_4 plants consumption is central to investigating animal ecology, agriculture, dietary transitions, and socio-environmental adaptations, and can be done using carbon isotope analysis. The conventional $\delta^{13}C$ threshold used to identify C_4 plant intake does not consider substantial ecological variability across Europe. By analyzing over 4,000 $\delta^{13}C$ values from archaeological C_3 and C_4 grains, we present a European-wide C_3 grain $\delta^{13}C$ baseline and establish adjusted $\delta^{13}C$ threshold estimations for C_4 consumption from the site to the ecozone scale using multicomponent environmental models and ecozone cluster analysis. We show that a fixed threshold lead to under- or overestimation of C_4 plant consumption, particularly in northern/humid and southern/arid regions, where the threshold needs to be revised downwards or upwards by up to 2‰. This refined framework offers a more accurate baseline for interpreting human and animal diet and enhances our understanding of the spread, adoption and consumption of C_4 crops across Europe.

Estimating the proportion of C_3 versus C_4 plants in human and animal diet is a key part of bioarchaeological, palaeontological and ecological research. Scholars worldwide have been investigating the spread of millet across Eurasia because this highly nutritious and drought-resistant C_4 plant can address various questions about past societies[1,2]. This includes complex social structures, the adoption of new subsistence strategies, the adaptation to challenging climatic and environmental settings, as well as mobility and health status[3–7]. In ecology and palaeontology, identifying C_3 and C_4 diets provides insight into (past) habitats, niche partitioning, and animal behaviours[8–12].

Stable carbon (C) isotope analyses—paired with nitrogen (N) isotope analyses when investigating collagen—represent the most efficient and preferred method to identify C_4 plant consumption from bioarchaeological and palaeontological skeletal remains. Due to different photosynthetic pathways between C_3 and C_4 plants, the ratio of $^{13}C/^{12}C$ isotopes (expressed as $\delta^{13}C$ in ‰) is significantly more negative in C_3 plants (−35 to −23‰) compared to C_4 plants (−14 to −10‰)[13–15]. Plant $\delta^{13}C$ is transferred to the consumer's body tissues along the food chain, following well-described and quantified fractionation processes[16,17], which leads to enriched $\delta^{13}C$ values in the tissues of C_4 plant consumers compared to C_3 plant consumers. In general, bone or dentine collagen $\delta^{13}C$ values above −18‰ and enamel or bone apatite $\delta^{13}C$ values above −10‰ indicate a mixed diet of C_3 and C_4 plants[13,18,19]. In contrast, $\delta^{13}C$ values above −12‰ and −4‰, respectively, represent a pure C_4 diet[13,18,19].

However, specific environmental and climatic settings influence the plant's $\delta^{13}C$ value[20]. For instance, C_3 plant $\delta^{13}C$ values are more depleted under oceanic or Mediterranean climates, forest soil, dense canopy, elevated humidity or increased CO_2 concentration[20,21]. Conversely, continental climate, aridity, salinity (including sea-spray effect), elevated temperature or high altitude tend to enrich plant $\delta^{13}C$ values, which are the basis of the terrestrial food chain[20,21]. The geographical location of the investigated site is also determinant. On average, skeletal tissues can be 1 to 2‰ lower in high latitudes compared to low latitudes in Europe[21–23]. Although C_4 plants react differently to environmental and climatic factors[14,24], their $\delta^{13}C$ values can vary across latitude as well[25,26]. This implies that the threshold value for C_4 plant consumption needs to be adapted depending on the geographical location and environmental settings to avoid misinterpretations of body tissue isotopic composition. This paper fills this research gap to avoid an over- or underestimation of C_4 plants dietary intakes of premodern animals and human communities across Europe.

The main research questions addressed here are: (i) In which regions of Europe is it required to apply an environmentally adjusted $\delta^{13}C$ threshold value for identifying C_3 versus C_4 plant consumption? (ii) What is the magnitude of this adjustment? (iii) Can we identify specific biogeographic parameters related to this isotope variability in Europe? This study draws on over 4000[27] published $\delta^{13}C$ values from charred archaeological C_3 and C_4 grains derived from Isotope-Ratio Mass Spectrometry (IRMS)[28–101]. We

[1]Faculty of History, Vilnius University, Vilnius, Lithuania. [2]Department of Environmental Sciences, University of Basel, Basel, Switzerland. [3]These authors contributed equally: Margaux L. C. Depaermentier, Michael Kempf. ✉e-mail: margaux.depaermentier@if.vu.lt; michael.kempf@unibas.ch

present an innovative and, to the best of our knowledge, unprecedented ecozone-based model framework that integrates multivariate environmental data to facilitate the identification of C_3 versus C_4 plant diets in bioarchaeological, palaeontological and ecological research.

Results

Ecozone cluster model

Using multicomponent environmental datasets from topographical and climatic variables, we applied *k*-means cluster analysis to determine zones of similar environmental conditions across Europe. The model provides 20 spatial clusters including one cluster with unclassified values where not all conditions were equally met (Figs. 1 and S1, Table 1). Due to numeric quantization of *k* observations, we labelled the clusters based on the percentiles of the respective data ranges using expressional combinations of temperature, climatic moisture index (CMI), and topography. Some of them are geographically restricted to specific regions, such as the cold and humid ecozones 4 and 5 in North-Eastern Europe, the mild and very humid ecozone 8 at the Atlantic coast, or the hot and arid ecozones in the south of Europe, northern Africa and the Near East (e.g., clusters 10, 16 and 18). Other ecozones are spatially more scattered, for example European high mountain ranges (e.g., clusters 11 and 15). The results can be compared to the biome-based ecoregions from the literature[102] despite the reduced number of modelled ecozones.

The sites from which the investigated grains originate cover 15 out of 20 modelled ecozones (Fig. 1, Supplementary data 1), representing most of the European geographical and ecological diversity. However, their distribution is biased by past and modern human activity, archaeological sampling and analytical strategies. Not all ecozones are equally represented in the sample and the ecozones 3, 12, 14, 15 and 18 were excluded from the analyses due to small sample sizes.

Isotope diversity among grain species

Despite the isotopic diversity between the main C_3 grain species included in this study (Fig. S2A, B, Supplementary data 2), the two dominant crops of this sample, i.e. the *Triticum* (wheat, n = 1923) and *Hordeum* (barley, n = 1843) species, are largely overlapping in the northern and southern parts of Europe (Fig. S2B, Supplementary data 2). Differences from the Central/Western European samples are mostly caused by the wide geographical area represented by this region. In the UK, however, the two crops show notably distinct $\delta^{13}C$ values (Fig. S2B, Supplementary data 2), which possibly reflects species-specific differences (e.g., the different timing of the vegetation period, which is earlier for barley, while wheat is more impacted by the summer

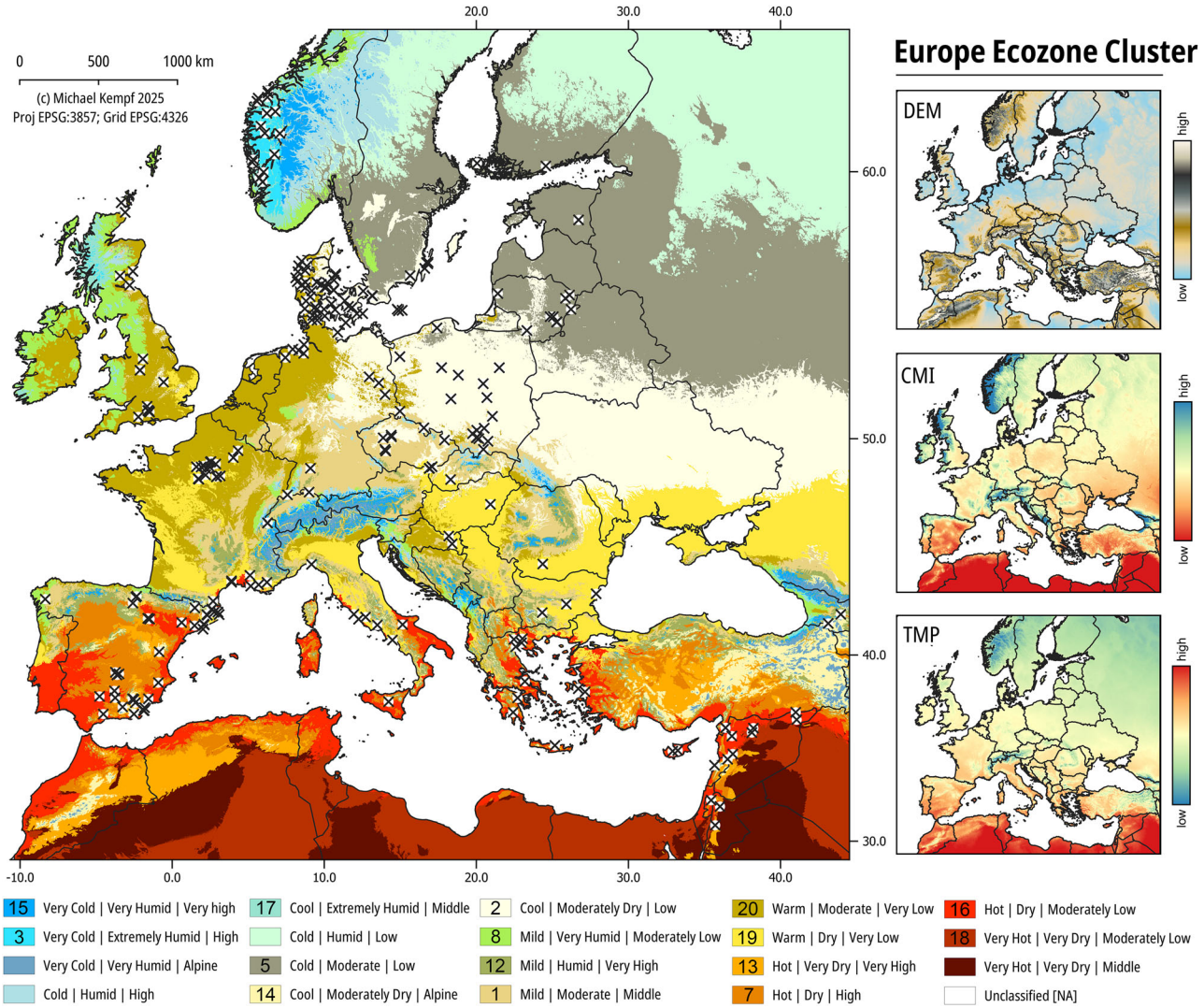

Fig. 1 | Site distribution over the European Ecozone clusters. 20 clusters based on temperature (TMP), moisture availability (CWB), and topography (DEM) were defined using *k-means* cluster analysis (with $k = 20$), including unclassified NA values (i.e., inland water). See the methods and material section for a description of the open source TMP, CWB and DEM data and their provenience. The sites are distributed over 15 clusters. See Table 1 for the ecozone descriptions and numbering and Fig. S1 for the ecozones displayed without sites. Figure by Michael Kempf, created using the open source R and QGIS software.

Table 1 | K-means cluster ecozone cluster summary table including description

cluster	mean TMP	mean CWB	mean DEM	SD TMP	SD CBW	SD DEM	Description (TMP|CWB|DEM)
1	0.429	0.405	0.205	0.039	0.017	0.021	Mild|Moderate|Middle
2	0.362	0.343	0.06	0.019	0.01	0.013	Cool|Moderately Dry|Low
3	0.111	1	0.343	0.053	0.05	0.056	Very Cold|Extremely Humid|High
4	0.116	0.429	0.065	0.02	0.007	0.015	Cold|Humid|Low
5	0.242	0.392	0.051	0.02	0.009	0.011	Cold|Moderate|Low
6	NA	NA	NA	NA	NA	NA	NA [unclassified|waterbody]
7	0.659	0.248	0.296	0.04	0.019	0.024	Hot|Dry|High
8	0.398	0.544	0.083	0.05	0.019	0.026	Mild|Very Humid|Moderately Low
9	0.115	0.51	0.296	0.051	0.022	0.03	Cold|Humid|High
10	0.938	0.012	0.269	0.039	0.017	0.027	Very Hot|Very Dry|Middle
11	0	0.521	1	0.065	0.051	0.058	Very Cold|Very Humid|Alpine
12	0.388	0.406	0.43	0.043	0.024	0.03	Mild|Humid|Very High
13	0.633	0.184	0.479	0.053	0.026	0.03	Hot|Very Dry|Very High
14	0.329	0.318	0.718	0.051	0.025	0.043	Cool|Moderately Dry|Alpine
15	0.091	0.584	0.579	0.07	0.035	0.042	Very Cold|Very Humid|Very High
16	0.799	0.226	0.092	0.032	0.021	0.027	Hot|Dry|Moderately Low
17	0.297	0.749	0.131	0.052	0.031	0.038	Cool|Extremely Humid|Middle
18	1	0	0.078	0.031	0.018	0.023	Very Hot|Very Dry|Moderately Low
19	0.53	0.306	0.045	0.034	0.012	0.015	Warm|Dry|Very Low
20	0.473	0.395	0.046	0.032	0.011	0.015	Warm|Moderate|Very Low

TMP temperature, *CWB* moisture availability, *DEM* digital elevation model (i.e., topography), SD: standard deviation. Cluster 6 represents unclassified water bodies (NA; −99999).

conditions)[28,103] or the environmental diversity of the fields used to grow the different crops[29]. Because human and animal diet is never based on one single crop, the C_3 grain sample was kept as one entity for the rest of the analyses. In contrast, the C_3 and C_4 grains show distinct $\delta^{13}C$ values (Fig. S3C, Supplementary data 2), as expected from their different photosynthetic pathways[13–15]. They are thus considered separately in the rest of the study.

Temporal isotope variability

Among the entire C_3 grains dataset, there is hardly any evolution of $\delta^{13}C$ over time (linear model [lm] $R^2 = 0.017$, p = 1.75e-17; Pearson's r value = 0.13, p = <2.2e-16; Fig. S3, Supplementary data 2). When distinguishing between the geographical subsets UK (lm $R^2 = 0.044$, p = 0.000276; Pearson's r value = −0.21, p = 0.000276), Southern (lm $R^2 = 0.03$, p = 3.43e-17; Pearson's r value = 0.17, p = <2.2e-16), Central/Western (lm $R^2 = 0.215$, p = 1.80e-32; Pearson's r value = 0.46, p = <2.2e-16) and Northern Europe (including Denmark: lm $R^2 = 0.078$, p = 4.13e-18; Pearson's r value = 0.28, p = <2.2e-16; and excluding Denmark: lm $R^2 = 0.059$, p = 1.55e-09; Pearson's r value = 0.34, p = <2.2e-16), the positive correlation between C_3 grain $\delta^{13}C$ values and the grain mean date is particularly weak (Fig. S4A–E, Supplementary data 2). In particular, the slightly stronger relationship observed for Central/Western Europe (Fig. S4B) is biased by the youngest samples from Central France, which exhibit particularly enriched $\delta^{13}C$ values (Fig. S4C). At the ecozone level, a weak to moderate and significant increase in C_3 grains $\delta^{13}C$ values can be observed for ecozone 1 (lm $R^2 = 0.359$, p = 5.39e-15; Pearson's r value = 0.60, p = 5.39e-15) and ecozone 17 only (lm $R^2 = 0.223$, p = 0.00157; Pearson's r value = 0.47, p = 1.57e-03) (Figs. 1 and S5, Supplementary data 2). The C_4 grains dataset has a small sample size and each geographical area is represented by short chronologies, which does not enable any proper diachronic analysis (Fig. S6A). The slight decrease in C_4 $\delta^{13}C$ values over time might thus be only considered statistically significant in Southern Europe despite the chronological gap of nearly a thousand years between the oldest and youngest cluster (Fig. S6B, Supplementary data 2). This implies that the C_3 and the C_4 grains datasets were not subdivided into different chronological phases for the subsequent analyses.

Geographical isotope variability

Splitting the C_3 grain dataset into geographical subsets (UK, Northern, Southern, and Central/Western Europe) shows that the median $\delta^{13}C$ value of C_3 grains from Northern Europe is approximately 1‰ lower than that from Southern Europe (Fig. 2A, Table 2). This confirms the previous observations made on different types of samples such as faunal remains[22,23] and modern plants[21]. Yet it has to be stressed that the standard deviation (1 SD) is quite large for both regions (±1.35 and ±1.05, respectively), implying some overlap. Despite the high latitude, C_3 grains from the UK exhibit among the highest $\delta^{13}C$ values across time (Figs. 2A and S4), which can be related to the oceanic climate[22,23]. In Denmark, the low $\delta^{13}C$ values of the oldest half of the sample (c. 3700–3000 BCE) shift to particularly enriched $\delta^{13}C$ values for the most recent half of the sample (c. 1000 BCE–1000 CE) (Fig. S7, Supplementary data 2). This might reflect changes in agricultural practices and soil management following its decrease in quality starting from the Neolithic period[30,31].

Using the whole dataset, we observe a significant decrease in C_3 grain $\delta^{13}C$ values with increasing latitude (Fig. 2B, Supplementary data 2). From the median values calculated for each latitudinal bin (Table 2, Fig. 2B), the C_3 grains $\delta^{13}C$ values from sites above 50° latitude are on average 0.54 to 1.72‰ lower than those of grains from sites at latitudes below 50° (Fig. 2B, Table 2). This confirms the mean offset of around 1–2‰ between Southern and Northern Europe. In comparison, there is a mean variation of 0.46‰ among the median $\delta^{13}C$ values of the latitudinal bins above 50° and approximately 0.33‰ among the median $\delta^{13}C$ values of the bins below 50°. The difference between southern and northern sites is therefore substantial, yet related to an increasing degree of variability towards the north. When excluding the UK and/or Denmark from this dataset due to the overall elevated values in these regions despite their northern latitude, the decrease in $\delta^{13}C$ values with increasing latitude is accordingly even stronger and more significant (Pearson's r value: −0.25 for the whole sample, −0.27 excluding UK and

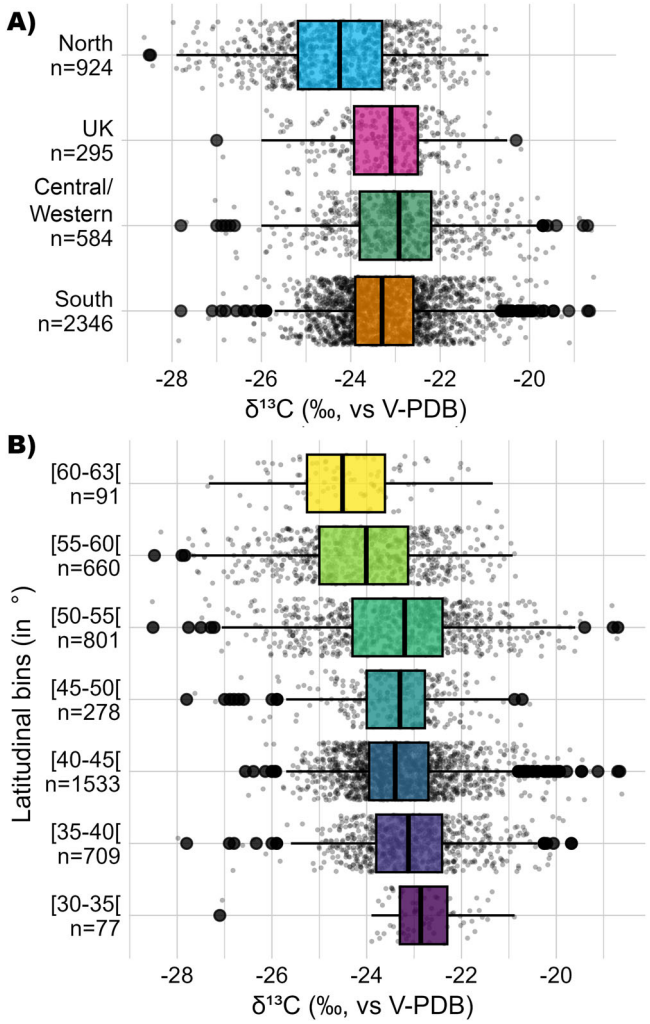

Fig. 2 | Geographical isotopic variability in C_3 grains. A C_3 grains $\delta^{13}C$ values in Europe. **B** C_3 grain $\delta^{13}C$ variability compared to latitudinal bins within Europe. The middle line of the box represents the median value, the box is delimited by the quartiles Q1 on the left and Q3 on the right and contains the middle half of the sample, the horizontal lines completed by the outlier dots represent the extent of the data. The mean, median, mean absolute deviation (MAD) and standard deviation (1 SD) values for each region and each latitudinal bin are listed in Table 2. The results of the one-way ANOVA tests related to (**A**) and (**B**) and of the Pearson's correlations related to the C_3 grain $\delta^{13}C$ versus latitude for the whole dataset and for specific subsets are reported in Supplementary data 2. Figure by Margaux L. C. Depaermentier, created using the open source R software.

−0.30 excluding UK and Denmark, with a p-value < 2.2e-16 in each case; see Supplementary data 2).

At the modern country level, the C_3 grains from Lithuania (median −25.18 ± 1.16‰, n = 153) are on average nearly 2.5‰ lower than those from Jordan (median −22.86 ± 0.74‰, n = 46) (Fig. 3A, Table 2) which exceeds the previously defined offset of 1–2‰ between Southern and Northern Europe[21–23]. On the contrary, the Jordan sample is on average 0.80‰ more enriched than those from Greece (median −23.50 ± 0.82‰, n = 383) or Italy (median −23.50 ± 0.97‰, n = 497) despite their shared southern location. Consequently, the North–South-dichotomy is not enough to characterize the different isotopic composition of grains from diverse parts of Europe and does not account for micro-regional environmental diversity. Moreover, the northernmost countries show standard deviations (SD) of 1.29‰ on average (1.12 to 1.67‰ in total), which is sensibly more than in most of the southern (from 0.40 to 1.43‰; mean: 0.92‰) and of the central/western countries (from 0.39 to 1.51‰, mean: 0.90‰) (see the ANOVA test in Supplementary data 2).

Similarly, the C_4 grain $\delta^{13}C$ values from Lithuania (median: −10.83 ± 0.48‰, n = 20) are on average nearly 1‰ lower than those from Greece (median: −10.19 ± 0.15‰, n = 12), France (median: −10.15‰, n = 16) or Poland (median: −10.19 ± 0.15‰, n = 9) (Fig. 3B, C; Table 2). The sample sizes from Spain (n = 3, median: −10.69 ± 0.15‰) and from the Czech Republic (n = 1) are too low to be considered representative. This trend confirms previous studies from China with depleted C_4 grain $\delta^{13}C$ values recorded at higher latitudes[25,26]. The pattern is further supported by the larger C_4 grain $\delta^{13}C$ dataset resulting from Alpha Magnetic Spectrometer (AMS) in Europe[104], showing generally lower $\delta^{13}C$ values in Northern compared to Southern or Central Europe (Fig. S8). However, AMS stable isotopic data lack precision due to differences in calibration compared to IRMS and provide particularly wide and unusual $\delta^{13}C$ ranges for C_4 grains[105]. Therefore, these data cannot be used to extend the IRMS dataset in this study. Differences in local plant genotypes are considered more likely triggers for the isotopic variability than climate and water availability[24]. Both C_3 and C_4 grains exhibit lower $\delta^{13}C$ values in some northern regions relative to the rest of Europe, leading to regional variation in the $\delta^{13}C$ threshold for identifying C_4 consumption.

Ecological isotopic variability

The geographical isotopic variability is related to environmental factors captured in the ecozone model. C_3 grain samples from Lithuania (n = 153), Estonia (n = 11), Finland (n = 44), and from parts of Denmark (n = 86) fall into the subhumid temperate lowlands of North-Eastern Europe represented by ecozone 5 (n = 294). Together with ecozone 17 (n = 42)—represented by grains from Norway only—these samples exhibit the lowest median $\delta^{13}C$ values (−25.01 ± 1.25‰ and −25.08 ± 1.20‰, respectively) for charred C_3 grains in Europe (Fig. 4, Table 2). The high humidity, low temperature and low to moderately elevated topography of these ecozones can explain the depleted $\delta^{13}C$ values[20]. Ecozone 20 (n = 717), represented by balanced temperate plains scattered over Europe and including samples mostly from Denmark, northern Germany and England, exhibit a much higher median $\delta^{13}C$ value (−23.00 ± 1.16‰) and its range hardly overlaps with the other northern samples. Beyond the influence of agricultural practices mentioned above[30,31], this can be explained by higher temperatures and moderate humidity characterizing this ecozone. In contrast, the 1007 samples from ecozone 17 and the 140 samples from ecozone 1 show the lowest median $\delta^{13}C$ values among the sites below 50° latitude (−23.47 ± 0.82‰ and −23.35 ± 1.41‰, respectively). This reflects the mild and moist conditions of these transition zones at a mid-range altitude. In Southern Europe, the ecozones 7 and 13, representing warm highlands in the Mediterranean area, show the highest median $\delta^{13}C$ values (−22.93 ± 1.35‰ and −22.56 ± 0.87‰, respectively), deriving from the drier and warmer climatic conditions. The ecozones 2, 8 and 19 are scattered over wide areas of Europe and are not related to extreme temperatures. Their isotopic ratios show intermediate values (Table 2). Ecozones 3, 12, 14, 15 and 18 cannot be included in this isotope investigation due to their small sample size.

Discussion

Building on the substantial geographical and ecological variation in isotope values within C_3 (and to a lesser extent C_4) plants, it is essential to revise the commonly used $\delta^{13}C$ threshold for identifying C_4 consumption, such as −18.0‰ for mammal collagen (for example, ref. 7). At each investigated site, the C_3 and C_4 grain $\delta^{13}C$ values from this dataset (Fig. 5A) were used to create theoretical collagen $\delta^{13}C$ values for a diet based exclusively on these crops (Fig. 5B)—which is no realistic diet for humans or animals and was only used for a first theoretical model. This resulted in site-specific estimations for an overall C_3 grain-based diet with 10% to 20% C_4 grain inputs (Fig. 5B and Supplementary data 1). Our model shows that at several sites from the Baltic and Nordic countries, human or animal collagen $\delta^{13}C$ values

Table 2 | Statistical summary for the C_3 and C_4 grain $\delta^{13}C$ values over the latitude bins, regions, modern countries and ecozones

Variable		n C_3 grains	Mean C_3 grain $\delta^{13}C$ (‰)	Median C_3 grain $\delta^{13}C$ (‰)	MAD for C_3 grain $\delta^{13}C$ (‰)	1 SD for C_3 grain $\delta^{13}C$ (‰)	Comment (C_3 grains)	n C_4 grains	Mean C_4 grain $\delta^{13}C$ (‰)	Median C_4 grain $\delta^{13}C$ (‰)	MAD for C_4 grain $\delta^{13}C$ (‰)	SD for C_4 grain $\delta^{13}C$ (‰)	Comment (C_4 grains)
Latitude bins (in °)	[30–35]	77	−22.82	−22.86	0.74	0.85		0					
	[35–40]	709	−23.07	−23.12	1.02	1.08		0					
	[40–45]	1533	−23.29	−23.40	0.89	1.03		18	−10.45	−10.49	0.44	0.31	
	[45–50]	278	−23.42	−23.30	0.89	1.06		13	−10.05	−10.00	0.30	0.36	
	[50–55]	801	−23.31	−23.20	1.44	1.47		19	−10.448421	−10.29	0.42	0.73	
	[55–60]	660	−24.10	−24.01	1.40	1.36		11	−10.95	−10.93	0.52	0.49	(ends at 55.69°)
	[60–63[	91	−24.44	−24.51	1.17	1.24		0					
Region	North	924	−24.26	−24.25	1.41	1.35		20	−10.88	−10.83	0.48	0.70	
	UK	295	−23.21	−23.10	1.04	1.06		23	−10.09	−10.19	0.30	0.31	
	Central/ West	584	−22.95	−22.92	1.16	1.30		0					
	South	2346	−23.21	−23.30	0.95	1.05		18	−10.45	−10.49	0.44	0.31	
Modern country	Andorra	3	−22.33	−22.10	0.37	0.62	small sample size	0					
	Bulgaria	22	−23.45	−23.50	0.44	0.40		0					
	Croatia	27	−23.64	−23.80	0.59	0.88		0					
	Cyprus	8	−22.97	−23.09	0.76	0.85	small sample size	0					
	Czech Republic	67	−23.14	−23.00	0.74	0.73		1	−9.90	−9.90	0.00	NA	small sample size
	Denmark	323	−23.56	−23.36	1.19	1.32		0					
	England	259	−23.14	−23.02	0.93	1.01		0					
	Estonia	11	−24.47	−24.50	1.93	1.67	rather small sample size	0					
	Finland	44	−24.14	−24.39	1.05	1.23		16	−10.19	−10.15	0.36	0.44	
	France	206	−23.17	−23.20	0.82	0.92		0					
	Georgia	20	−21.87	−21.60	1.11	1.43		0					
	Germany	302	−22.62	−22.60	1.33	1.51		0					
	Greece	383	−23.50	−23.50	0.76	0.82		12	−10.32	−10.19	0.15	0.27	
	Hungary	4	−24.20	−24.25	0.15	0.22	small sample size	0					
	Italy	497	−23.38	−23.50	0.89	0.97		0					
	Jordan	46	−22.66	−22.86	0.82	0.74		0					
	Lebanon	2	−25.45	−25.45	2.45	2.33	small sample size	0					
	Lithuania	153	−25.13	−25.18	1.01	1.16		20	−10.88	−10.83	0.48	0.70	
	Norway	63	−24.82	−24.85	1.33	1.22		0					
	Poland	52	−23.84	−23.90	1.12	0.94		9	−10.16	−10.19	0.15	0.25	small sample size
	Scotland	36	−23.73	−23.90	1.48	1.24		0					
	Slovakia	10	−23.66	−23.50	0.44	0.39	rather small sample size	0					
	Spain	965	−23.08	−23.22	1.08	1.17		3	−10.66	−10.69	0.15	0.15	small sample size
	Sweden	327	−24.46	−24.50	1.19	1.12		0					
	Switzerland	7	−23.97	−24.10	0.30	0.46	small sample size	0					
	Syria	144	−23.07	−22.98	0.77	1.02		0					
	Turkey	168	−23.11	−23.12	0.79	0.83		0					
Ecozone cluster	1	140	−23.48	−23.35	1.42	1.41		8	−10.34	−10.44	0.37	0.49	small sample size
	2	511	−23.79	−23.80	1.33	1.41		10	−10.13	−10.19	0.15	0.25	rather small sample size

Table 2 (continued) | Statistical summary for the C_3 and C_4 grain $\delta^{13}C$ values over the latitude bins, regions, modern countries and ecozones

Variable		n C_3 grains	Mean C_3 grain $\delta^{13}C$ (‰)	Median C_3 grain $\delta^{13}C$ (‰)	MAD for C_3 grain $\delta^{13}C$ (‰)	1 SD for C_3 grain $\delta^{13}C$ (‰)	Comment (C_3 grains)	n C_4 grains	Mean C_4 grain $\delta^{13}C$ (‰)	Median C_4 grain $\delta^{13}C$ (‰)	MAD for C_4 grain $\delta^{13}C$ (‰)	SD for C_4 grain $\delta^{13}C$ (‰)	Comment (C_4 grains)
	3	4	−24.62	−24.69	1.25	1.07	small sample size	0					
	5	294	−24.96	−25.01	1.09	1.25		20	−10.88	−10.83	0.48	0.70	only Lithuania
	7	338	−22.83	−22.93	1.22	1.35		0					
	8	29	−24.18	−23.76	0.83	1.17		0					
	12	3	−22.33	−22.10	0.37	0.62	small sample size	0					
	13	86	−22.62	−22.56	0.94	0.87		0					
	14	6	−21.32	−21.30	0.67	0.64	small sample size	0					
	15	5	−20.88	−21.10	1.04	1.50	small sample size	0					
	16	964	−23.15	−23.20	0.95	1.01		12	−10.32	−10.19	0.15	0.27	rather small sample size
	17	42	−24.97	−25.08	1.48	1.20		0					
	18	3	−21.97	−22.10	0.15	0.32	small sample size	0					
	19	1007	−23.47	−23.50	0.74	0.82		11	−10.21	−10.10	0.30	0.42	rather small sample size
	20	717	−23.03	−23.00	1.05	1.16		0					

The values indicated for small sample sizes are considered non-representative for the related category.

below −19.0‰ (with a mean SD of 0.59‰)—and up to −19.68 ± 0.94‰ at Bėlis lake, Lithuania (n = 10), for example—already reflect a low C_4 input within a primarily C_3-grain-based diet. In the Mediterranean, the same C_4 input would result in collagen $\delta^{13}C$ values above −17.0 ± 0.77 or −16.0 ± 0.57‰ (Fig. 5B and Supplementary data 1).

It is generally accepted that at least 20% of dietary protein from an alternative source (such as C_4 compared to C_3 crops) is required to be detected in collagen[106]. However, with a model based on theoretical grain-based diets, a 20% C_4 input produces excessively elevated $\delta^{13}C$ estimates for mammal collagen (Supplementary data 1). This highlights the limits of a model based on non-realistic grain-based diets, as despite the important role of grains in human diet, both humans and animals have more varied diets in reality—the latter even consuming mostly other parts of the plant and only rarely grains. And with collagen $\delta^{13}C$ values reflecting the protein component of the diet[16], plant intake contributes less to collagen isotopic composition than animal-derived proteins, which may alter this threshold value in omnivorous diets. Moreover, in regions where the diet includes significant proportions of mushrooms[107], forest-derived foods influenced by the canopy effect[108,109], and/or freshwater fish[110–112], consumers are exposed to more depleted $\delta^{13}C$ values. These foods have a much stronger influence on collagen $\delta^{13}C$ values than any enrichment from C_4 plants. And since such conditions are highly plausible in the Baltics and in Scandinavia, the threshold $\delta^{13}C$ value for C_4 consumption might be even lower than those suggested by the model with 10% C_4 input (Figs. 5A, B and 6). On the contrary, potential marine food consumption[17] or sea-spray effects in coastal areas[113] need to be considered to avoid any over-estimation of C_4 plant intake.

A model involving all other food resources would go beyond the scope of this paper. But to accurately estimate the actual local threshold values for C_4 consumption, it is essential to use $\delta^{13}C$ and $\delta^{15}N$ values from as many local and contemporaneous food resources as possible, including crops (for example[32]). Wild plants would further represent a better baseline for herbivore's diets. Yet these are much more seldom in archaeological remains and their isotopic ratios are hardly represented in bioarchaeological studies so far. A model based on modern plants[21] or on tree $\delta^{13}C$ values[114] can thus further serve as comparison $\delta^{13}C$ baseline for herbivore's diets. The combination of various isotope systems[113,115,116] and/or the application of mixing models[117] are further powerful approaches to disentangle the diverse dietary sources.

Considerable isotopic variability is observed within each site, region and ecozone (Figs. 2–4 and 5A, Supplementary data 1–2), indicating that a range rather than a sharp threshold value is more appropriate (Figs. 5B and 6B). This isotopic variability is not only related to the gradual and complex variation of environmental settings across Europe, but is also intrinsic to the grains, as grain $\delta^{13}C$ may vary for up to 0.5‰ within one ear despite same species and same growing conditions[33]. Differing growing conditions, in particular various watering practices, can further impact local grain $\delta^{13}C$ values by up to 1.7‰[24,28]. Wild plants $\delta^{13}C$ values may be good comparison references to disentangle anthropogenic and natural differences in water regimes[21,118,119]. Another variability might be induced by diverging analytical uncertainty between datasets, as the data result from different laboratories and protocols and were obtained with different calibrations—which are relevant information to make sure that the datasets are comparable[120]. Unfortunately, information on calibration, precision and accuracy of the published isotope data were mostly missing, thus it was not possible to assess the impact on the presented results. Yet when available, the error value for replicated samples was very low and still within the range of analytical errors.

An evolution of the grain $\delta^{13}C$ values might be expected over time as well, especially when considering the various climatic phases that implied a great variation in moisture and temperature throughout Europe over the investigated time frame. The presented regional differences in grain $\delta^{13}C$ values have therefore varied between the climatic phases (Fig. S10), yet the isotopic variations within each region over the various climatic phases is overall significantly weak (Supplementary data 2). A larger dataset for the most recent periods might reveal more effective trends. In this study, the

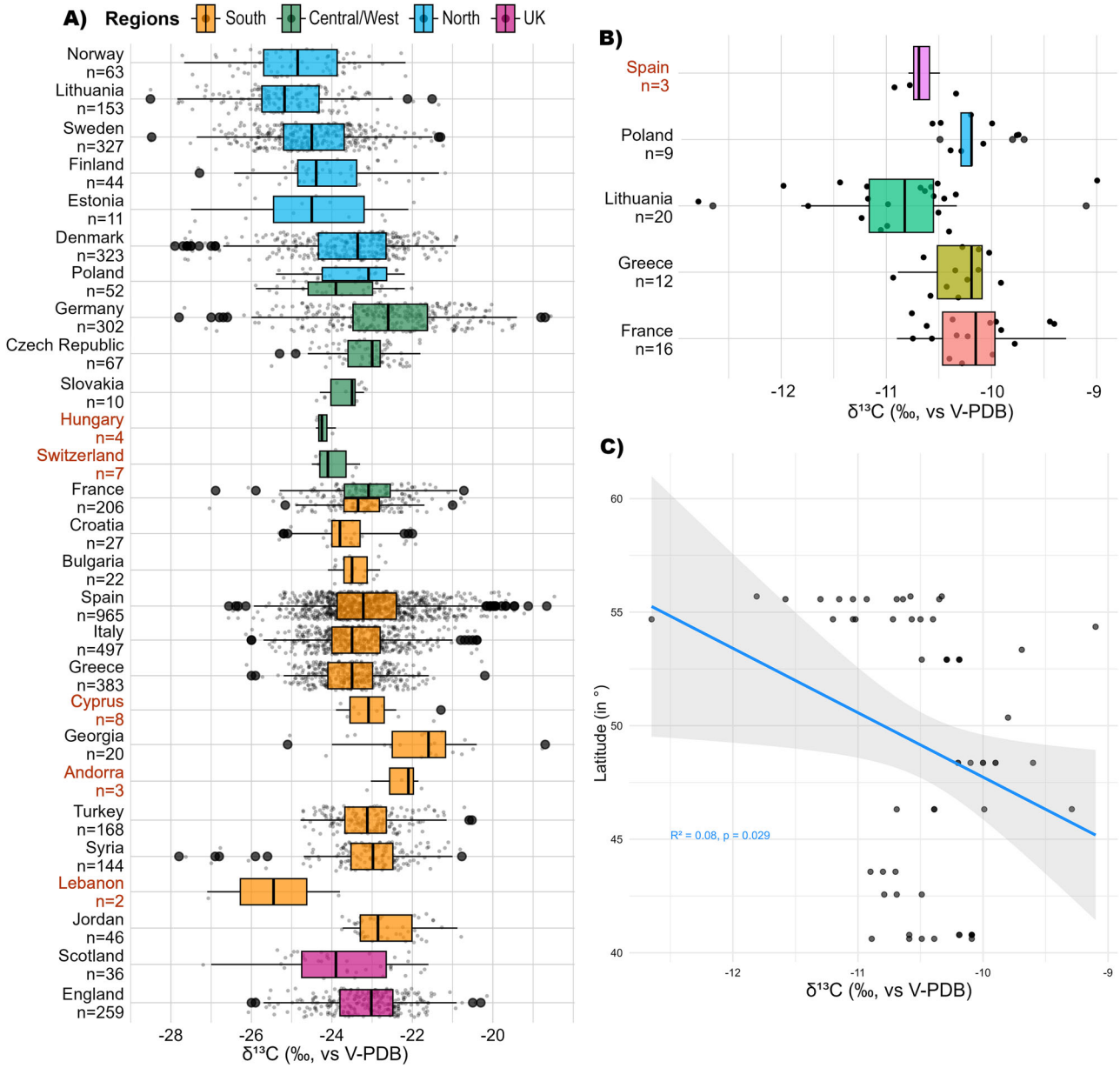

Fig. 3 | Differences in archaeological charred C_3 and C_4 grain $\delta^{13}C$ values in Europe. A C_3 grain $\delta^{13}C$ values over the modern countries. **B** C_4 grain $\delta^{13}C$ values over modern countries. **C** The comparison between latitude and C_4 grain $\delta^{13}C$ values shows a weak but significant negative correlation. Boxplots are defined in Fig. 2. The mean, median, MAD and SD values for each modern country are listed in Table 2. The results of the related one-way ANOVA tests and Pearson's correlations are available from Supplementary data 2. The red labels show non-representative sample sizes (n < 10). Figure by Margaux L. C. Depaermentier, created using the open source R software.

impact of the chronological depth and imbalance covered by this dataset can be considered weak (Figs. S2–S5 and S10).

The isotopic difference reported in this study between regions and ecozone therefore remains strong enough to highlight environmentally-driven differences (Figs. 2–7, Table 2) even from grains that were possibly undergoing various cultivation practices. Our approach thus demonstrates that the threshold at −18.0‰ for consumer's collagen is not universal and is mostly valid in the ecozone 2 (−17.51 ± 1.28‰), whereas the northern ecozone 5 and the widespread ecozone 17 require a threshold $\delta^{13}C$ value closer to −19.0‰, i.e., −18.59 ± 1.12 and −18.67 ± 1.08‰, respectively. In high-temperature Mediterranean lowlands (ecozone 16), European plains (ecozone 19), and Atlantic regions (ecozone 20), the threshold shifts to −17.0‰ (i.e., −16.88 ± 0.90‰, −17.15 ± 0.74‰, and −16.71 ± 1.05‰, respectively; Figs. 6, 7, Tab. S1). In the arid southern regions (ecozone 13 [−16.31 ± 0.78‰], and partially ecozones 7 and 16), it approaches −16.0‰ (Fig. 7, Tab. S1). Yet in each case, the SD ranges from 0.74 to 1.26‰, stressing again the isotopic variability within ecozones.

To conclude, this paper offers both a European-wide $\delta^{13}C$ baseline from archaeological charred C_3 grains and a threshold-value-model for environmentally adjusted identification of C_4 consumption from the site to the ecozone level across Europe (Fig. 7, Tab. S1). The grain baseline offers the advantage to consider a fundamental dietary resource (in particular for humans) as reference data and can be completed by local foods resources at the site level for more holistic and accurate interpretations. A comparison to wild proxies further enhances the results for animal diets. The threshold estimations are particularly suitable in bioarchaeological, ecological or palaeontological studies for which local plants or food resources are unavailable for calculating an isotopic baseline. However, it requires to account for the great degree of isotopic variability within each geographical entity as underlined by the SD values—a variability slightly increasing with latitude.

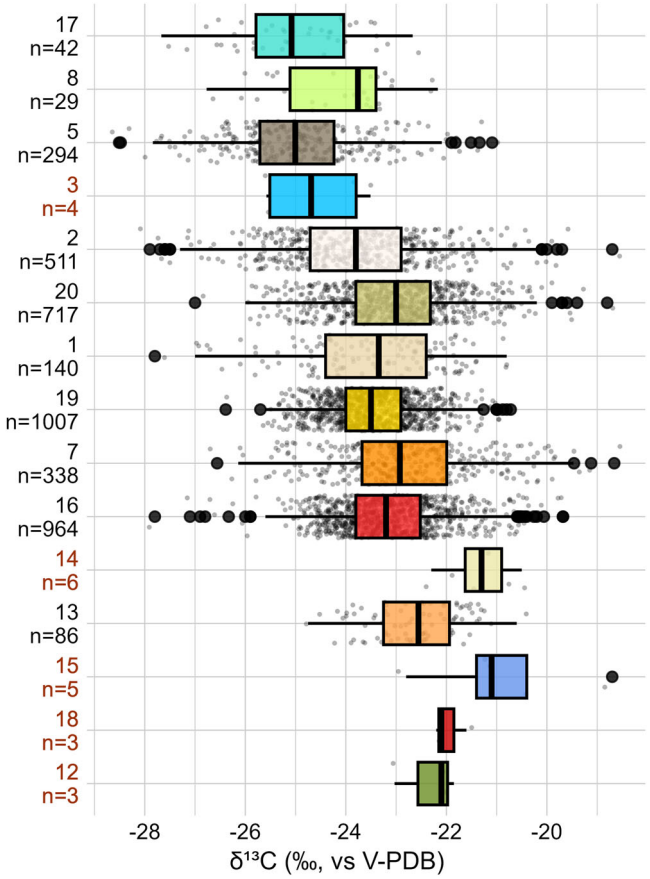

Fig. 4 | C_3 grains $\delta^{13}C$ values over the European ecozones clusters. The ecozone numbers refer to the numbering in Table 1. Boxplots are defined in Fig. 2. The boxplots are ordered from top to bottom according to decreasing latitude and to increasing temperature within the ecozone. The red labels underline non-representative sample sizes (n < 10). The mean, median, MAD and SD values for each ecozone can be found in Table 2. The results of the one-way ANOVA test are available from Supplementary data 2. Figure by Margaux L. C. Depaermentier, created using the open source R software.

In this context, the point-based approach (Fig. 5) provides more accurate yet geographically discrete data, while the interpolation-based approach (Fig. 6) offers ecologically sensitive estimates over large areas at the ecozone level, both related to some degree of uncertainty or variability. Future datasets could be used to test (and if necessary adjust) the interpolated values in areas of currently low site density. This innovative and context-sensitive ecozone clustering model based on temperature, humidity, and elevation thus enables more accurate interpretations of both animal ecologies and anthropogenic social and agricultural dynamics across Europe by avoiding over- or underestimation of C_4 consumption.

Methods and material

Isotopic dataset

The material used in this study consists of published $\delta^{13}C$ values from charred grains derived from archaeological context, compiled into one single dataset[27]. The data was collected from 75 publications until September 2025[28–101], also using the open access online repositories IsoArch[121], MAIA[122], Isotòpia[123], IsoMedIta[124] and CIMA[125]. In total, this represents 4,210 $\delta^{13}C$ values of C_3 and C_4 grains derived from 260 sites dated between 8000 BCE and 1800 CE. The represented C_3 plants are oat (*Avena species*, n = 58), rye (*Secale species*, n = 325), barley (*Hordeum species*, n = 1843), and wheat (*Triticum species*, n = 1923). Broomcorn millet (*Panicum miliaceum*, n = 57) and foxtail millet (*Setaria italica*, n = 4) represent the C_4 crops from this dataset. To facilitate visualization and pattern-recognition, the C_3 and C_4 grain datasets were considered separately for the various analyses due to their distinct $\delta^{13}C$ values and due to the particularly small C_4 grain sample size. C_3 and C_4 grain $\delta^{13}C$ values were then combined to address the question of identifying the introduction of C_4 crops in C_3 plants-based diets. Despite the fact that anthropogenic agricultural practices such as irrigation can impact grain $\delta^{13}C$ values[24,28], altering the natural and ecological signal, crops remain an important proxy for human diet regardless of agricultural practices, as their isotopic composition would be transferred to human tissues all the same. The ecological differences are considered important enough across Europe to be detectable from grain isotopic composition despite anthropogenic alterations. Wild plants would have represented a better proxy for animal diet, however, this proxy is lacking from archaeological contexts—or could be derived from tree $\delta^{13}C$ values for the most recent periods[114].

Geographically, the research area spans modern Europe and the Mediterranean countries of the Near East, i.e., between 30 and 63° (N) latitude and between −8 and 45° (E) longitude. Yet the data is not evenly distributed and Denmark is over-represented in terms of sites, while Greece is over-represented in terms of number of samples. There are considerable gaps in several regions of Europe (see Fig. 1 and the isotopic dataset[27]). Chronologically, this dataset covers most archaeological and historical periods and ranges from 8000 BCE to 1800 CE. In this context, it is important to stress that the oldest samples (8000–6000 BCE) exclusively originate from Greece, whereas samples from Northern Europe are predominantly younger than 1000 BCE—except for some larger site samples dated between 4000 BCE and 2000 BCE. Modern data created in the framework of experimental archaeology were not included in the dataset because of the controlled conditions in which they were produced and because of the different present-day atmospheric composition compared to pre-industrial periods[126].

Only data obtained from Isotope-Ratio Mass Spectrometry (IRMS) were selected for analyses. Despite the fact that these values are not comparable to IRMS isotopic values due to different calibrations[105], a European-wide dataset obtained from Accelerator Mass Spectrometry (AMS) in the context of radiocarbon measurements[104] was also used as a comparison dataset to verify whether the same trend is visible among both datasets. Importantly, grain $\delta^{13}C$ values are sometimes (i.e., in 12 out of 64 publications used in this study) published in form of corrected values to consider the charring effect on the carbon isotope composition of archaeological C_3[127,128] and C_4 grains[129,130]. But following the approach by Gron et al.[30], we are considering here only uncorrected values in order to enhance the comparability between datasets. This is considered to have no significant impact on this study's results, as the charring effect is not systematic[33] particularly low on grain $\delta^{13}C$ values (i.e., 0.06 to 0.18‰[33,127–130] on C_3 and C_4 grains for a heat up to 300 °C) and remains below analytical errors for isotope analyses[131].

Statistical analyses

All statistical analyses were performed using R software[132] and the results and relevant values are summarised in Supplementary data 2. To determine the relationship between grain $\delta^{13}C$ values and chronology or geographical location, we applied both Pearson's correlation tests and linear models—the latter using the *lme4* package[133]. The Pearson correlation coefficient (Pearson's r value) indicated the strength and direction of a linear relationship between two tested variables, the confidence interval gives the uncertainty range for the true correlation. While in the linear model, the R-squared values show the percentage of the dataset affected by the relationship and the p-values show the significance of the results. To determine the geographical scale at which significant changes in grain values occur, the dataset was divided into various bins. At the largest scale, the main regions of Europe, split into Northern Europe, Southern Europe, Central/Western Europe and the UK. This is not only convenient but also follows expectations based on previous research[21–23]. At the smallest geographical scale, the dataset was binned according to the borders of modern countries. Boxplots were used for data visualization and one-way ANOVA tests were performed to test the

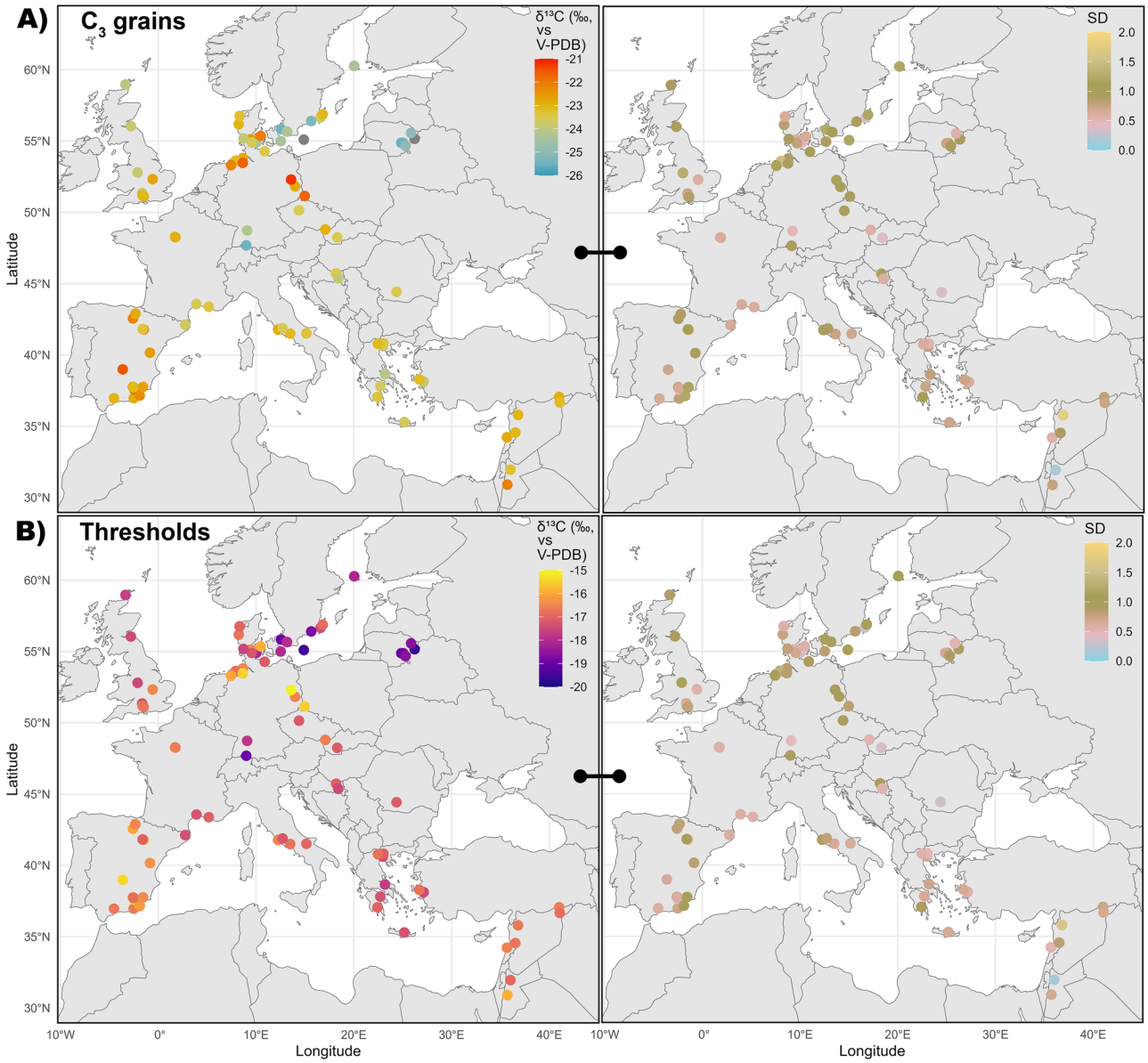

Fig. 5 | Point-based approach for baseline C_3 grain $\delta^{13}C$ values and estimated threshold values for C_4 diet identification in mammal collagen at sites with n ≥ 10 grains. **A** Median C_3 grain $\delta^{13}C$ values (left) and related SD (right). **B** Median estimated threshold $\delta^{13}C$ values for mammal collagen (left) and related SD (right) based on a theoretical 100%-grain-based-diet. The mean, median, SD and MAD values for each site are listed in Supplementary data 1. The same maps including even site with n < 10 are in Fig. S9. Figure by Margaux L. C. Depaermentier, created using the open source R software.

difference in grain $\delta^{13}C$ values between the investigated clusters. The results and relevant values for the ANOVA tests are summarised in Supplementary data 2). Because our dataset shows a particularly important isotopic variability, the results for each considered bin or entity/group are presented in the text using the median value (since the mean value is more sensitive to extreme outliers) and the related one standard deviation (1 SD). The tables are showing the mean, median, median absolute deviation (MAD) and 1 SD for each category/bin. In order to integrate an ecological dimension to the investigation of grain $\delta^{13}C$ variability, the dataset was also binned into newly determined ecozones, as presented in the section below.

Environmental cluster

For the cluster analysis, we used these R-packages: *terra*[134], *sf*[135,136], *gtools*[137], *dplyr*[138] and *ggplot2*[139], *ggspatial*[140], *gridExtra*[141] for plotting, as described in the R-code provided in the open access repository to this paper[142]. We used an unsupervised *k*-means clustering approach based on three spatial predictors to differentiate environmental ecozones across Europe. Components include elevation (DEM), mean temperature (T), and the Climatic Moisture Index (CMI). A DEM derived from the USGS (United States Geological Survey, Global Multi-resolution Terrain Elevation Data 2010, https://earthexplorer.usgs.gov/; last accessed 19th of June 2025). Monthly resolved climate variables for the period 1980-2018 were downloaded from CHELSA[143]. The CMI represents a standardized water availability index, calculated as the ratio of precipitation (P) to potential evapotranspiration (PET) with CMI = P − PET. We used CHELSA v2.1 monthly CMI data based on the Penman-Monteith equation for PET and downscaled from ERA5 reanalysis. The grids were reprojected to a meter-based projection (EPSG:3857) and cropped to the extent of the geographic European landmass. The dataset (n = 468) were aggregated to a 1000 m resolution using bilinear interpolation prior to clustering. Monthly layers were averaged to create a multiannual mean (1980–2018). To allow comparison between variables with different scales and units, all raster layers were standardized using z-score normalization with mean and standard deviation (sd) of the raster (z = cell value − mean_raster / sd_raster). A regular grid of 1 km

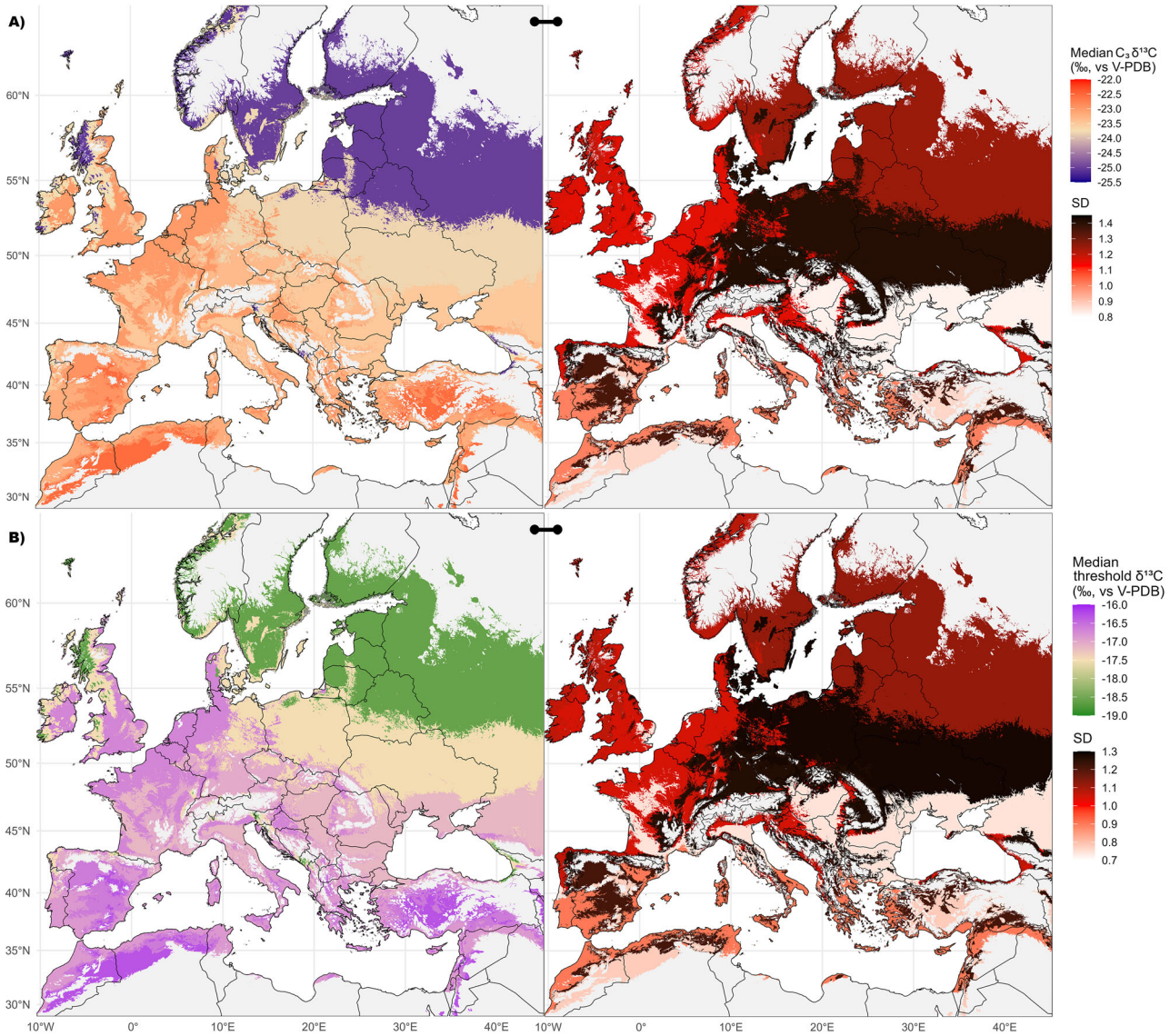

Fig. 6 | Ecozone-based interpolation of the C_3 grain $\delta^{13}C$ baseline and of the estimated threshold $\delta^{13}C$ values for detecting C_4 consumers. A Median $\delta^{13}C$ (left) and SD values (right) of charred C_3 grains interpolated at the ecozone level. **B** Median $\delta^{13}C$ (left) and SD values (right) of the estimated threshold ranges for C_4 consumption for each ecozone. Ecozones 3, 12, 14, 15 and 18 are left grey due to their too small sample sizes. Ecozones 4, 9, 10, 11 and 15 are left grey due to the absence of data. The ecozone's mean, median, SD and MAD values for C_3 grains and for C_4 consumption are listed in Table 2 and Tab. S1, respectively. Figure by Michael Kempf, created using the open source R and QGIS software.

spacing was generated across the study area and the centroid of each grid cell was calculated for regular point sampling. To reduce edge effects and avoid NA values near the coast, centroids were restricted to land areas using a simplified buffer around the European landmass boundaries. At each centroid location, the values were extracted from the normalized rasters.

K-Means clustering

K-means clustering was performed using the extracted values, with the determined number of clusters $k = 20$. This dimensionality was chosen to balance regional ecological resolution with model interpretability, including NA values (replaced by −99999 during the cluster analysis to protect correct geographical raster reassignment). Each centroid was assigned a cluster label based on the combined environmental profile of elevation, temperature, and moisture availability. Cluster labels were spatially joined to centroid coordinates and rasterized back into a continuous spatial layer using the DEM grid as a template. The resulting map classifies observational sites into discrete clustered ecozones (Fig. 1).

To characterize each of the 20 ecozone clusters based on the data variability, we summarized the environmental properties of each cluster using the mean and standard deviation of the three input variables: Elevation (ELEV), T, and CMI. All values were normalized using z-scores prior to clustering, enabling direct comparison across variables. The clusters were then qualitatively interpreted based on their relative environmental signatures. For example, clusters with low temperatures, moderately dry conditions and high elevations were categorized as Cool|Moderately Dry|Alpine zones. Clusters with high temperatures and low moisture availability in low areas were described as Very Hot|Very Dry|Moderately Low. Intermediate clusters were labeled based on transitional or temperate climate conditions (Table 1).

Determining consumer's $\delta^{13}C$ values

To determine the theoretically expected $\delta^{13}C$ values of consumer tissues from a mixed C_3-C_4 diet, we first associated each C_3 grain $\delta^{13}C$ value to a measured or assumed C_4 grain $\delta^{13}C$ value. This means that for each site at

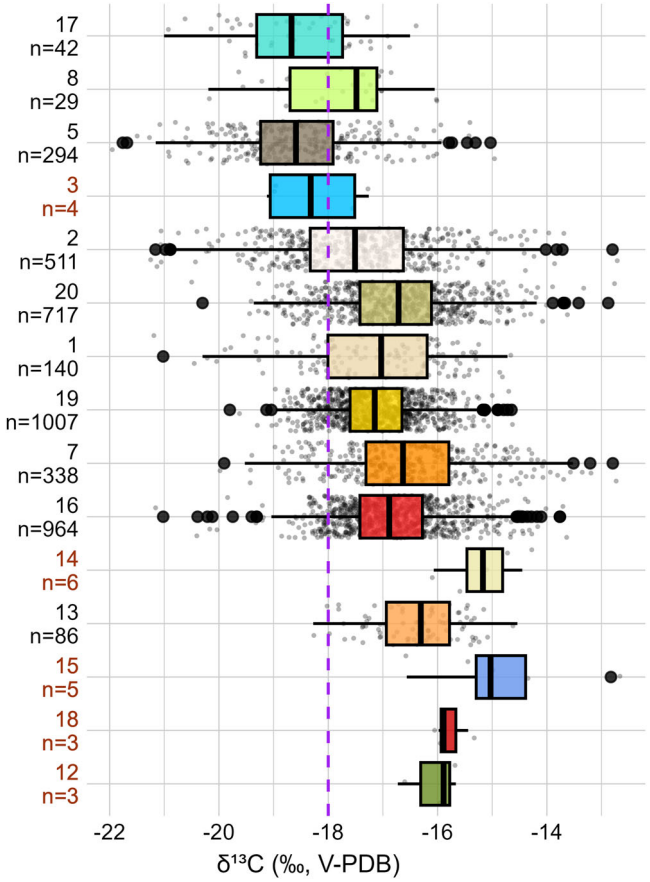

Fig. 7 | Theoretical $\delta^{13}C$ threshold ranges for C_4 consumption across the European ecozone clusters. The ecozone numbers refer to the numbering in Table 1. Boxplots are defined in Fig. 1. The boxplots are ordered from top to bottom according to decreasing latitude and to increasing temperature within the ecozone. The red labels underline non-representative sample sizes (n < 10). The mean, median, MAD and SD values for each ecozone are listed in Tab. S1. The purple line represents the revised $\delta^{13}C$ threshold value for C_4 consumption in mammal collagen (i.e., −18.0‰). Figure by Margaux L. C. Depaermentier, created using the open source R software.

which $\delta^{13}C$ values of both C_3 and C_4 grains were available, each C_3 grain $\delta^{13}C$ value got associated with the mean C_4 grain $\delta^{13}C$ value of the site. However, most of the sites included in this study provided no C_4 grain. In this case, a theoretical C_4 grain $\delta^{13}C$ value was determined for the site based on the observed values from this dataset. In most regions of Europe, the C_4 grain $\delta^{13}C$ value is thus expected to be −10‰[32,72,87]. Yet we observed that the C_4 grain $\delta^{13}C$ values in Lithuania—and by extension presumably in the northernmost latitudes of Europe—were rather around −11‰[68]. Similarly, C_4 grain $\delta^{13}C$ values from the western Mediterranean area seem to be closer to −10.5‰[35,47]. These regional values were thus used as theoretical C_4 grain $\delta^{13}C$ values associated with the measured C_3 grain $\delta^{13}C$ values at each site lacking C_4 grains (see summary in Supplementary data 1).

In a second step, 5‰ was added to each measured or theoretical grain $\delta^{13}C$ value to mimic the fractionation offset that applies between the diet and the consumer's collagenous tissues after consumption[16,17]. We applied this to both C_3 and C_4 grains, resulting in theoretical end-members collagen $\delta^{13}C$ values for 100% C_3 and 100% C_4 based diet, respectively. In a third step, we used these end-members values for each grain to create theoretical collagen $\delta^{13}C$ values for a C_3-grain-based diet including either 10% or 20% C_4 grains. These three first steps were done at the grain level to minimize the loss of resolution and information when working with mean values. In a fourth step, we eventually calculated a mean $\delta^{13}C$ value for these two types of diet at the site level (Supplementary data 1). It is fundamental to note that these fictitious diets based on 100% grains are not existing in nature and only represent a theoretical model using grains only.

Because a 100% grain-based diet does not exist in nature, the model using 10% of C_4 input was considered the most reliable basis for estimating the related collagen $\delta^{13}C$ values with low C_4 input in a normal mixed diet. These results are presented at the site-level to account for local variability in threshold $\delta^{13}C$ values for C_4 consumption (Fig. 5). The ecozone cluster model was used to create a map of interpolated threshold $\delta^{13}C$ values for C_4 consumption and hence suggest environmentally adjusted threshold $\delta^{13}C$ values for C_4 consumption (Fig. 6C). The European background maps used to create Figs. 5 and 6 are vector map data from https://www.naturalearthdata.com/, implemented using the package *rnaturalearth* in R-Software[132,144].

Materials & correspondence

The corresponding authors are MLCD and MK. The isotopic dataset used in this study is available from the open access repository: Depaermentier, M. L. C. (2025). Isotopic Dataset to: Depaermentier, MLC, Kempf, M, Motuzaitė Matuzevičiūtė, G. "Environmentally adjusted $\delta^{13}C$ thresholds for accurate detection of C_4 plant consumption in Europe" [Data set]. In Communications Earth & Environment. Zenodo. https://doi.org/10.5281/zenodo.17571650 [ref. 27 in this paper]. The data to reproduce the ecozone clusters is available from this open access repository: Kempf, M. (2025): Related files to: Depaermentier, MLC; Kempf, M; Motuzaitė Matuzevičiūtė, G: Environmentally adjusted $\delta^{13}C$ thresholds for accurate detection of C_4 plant consumption in Europe (2025) [Data set]. Zenodo. https://doi.org/10.5281/zenodo.15695070 [ref. 147 in this paper]. Climate variables used in this article are freely available from Karger et al. (2017): https://chelsa-climate.org/ (last accessed 19th of June 2025) [ref. 143 in this paper]. The Digital Elevation Model (DEM) can be downloaded from the USGS earthexplorer server: https://earthexplorer.usgs.gov/, last accessed 19th of June 2025.

Reporting summary

Further information on research design is available in the Nature Portfolio Reporting Summary linked to this article.

Data availability

The compiled isotopic dataset used in this study is available from the open access repository: Depaermentier, M. L. C. (2025). Isotopic Dataset to: Depaermentier, MLC, Kempf, M, Motuzaitė Matuzevičiūtė, G. "Environmentally adjusted $\delta^{13}C$ thresholds for accurate detection of C_4 plant consumption in Europe" [Data set]. In Communications Earth & Environment. Zenodo. https://doi.org/10.5281/zenodo.17571650 [ref. 27 in this paper]. The data to reproduce the ecozone clusters is available from this open access repository: Kempf, M. (2025): Related files to: Depaermentier, MLC; Kempf, M; Motuzaitė Matuzevičiūtė, G: Environmentally adjusted $\delta^{13}C$ thresholds for accurate detection of C_4 plant consumption in Europe (2025) [Data set]. Zenodo. https://doi.org/10.5281/zenodo.15695070 [ref. 147 in this paper]. Climate variables used in this article are freely available from Karger et al. (2017)[143]: https://chelsa-climate.org/ (last accessed 19th of June 2025). The Digital Elevation Model (DEM) can be downloaded from the USGS earthexplorer server: https://earthexplorer.usgs.gov/, last accessed 19th of June 2025.

Code availability

The code to reproduce the ecozone clusters is available from this open access repository: Kempf, M. (2025): Related files to: Depaermentier, MLC; Kempf, M; Motuzaitė Matuzevičiūtė, G: Environmentally adjusted $\delta^{13}C$ thresholds for accurate detection of C_4 plant consumption in Europe (2025) [Data set]. Zenodo. https://doi.org/10.5281/zenodo.15695070 [ref. 147 in this paper].

Received: 13 July 2025; Accepted: 12 November 2025;
Published online: 18 December 2025

References

1. Ventresca-Miller, A. R. et al. Adaptability of millets and landscapes: ancient cultivation in North-Central Asia. *Agronomy* **13**, 2848 (2023).
2. Motuzaitė Matuzevičiūtė, G. Broomcorn millet: from the past to the future. *AFF* **2**, 177–198 (2025).
3. Hakenbeck, S. E., Evans, J., Chapman, H. & Fothi, E. Practising pastoralism in an agricultural environment: an isotopic analysis of the impact of the Hunnic incursions on Pannonian populations. *PloS One* **12**, e0173079 (2017).
4. Kaupová, S. et al. Dukes, elites, and commoners: dietary reconstruction of the early medieval population of Bohemia (9th–11th Century AD, Czech Republic). *Archaeol. Anthropol. Sci.* **11**, 1887–1909 (2019).
5. Martin, L. et al. The place of millet in food globalization during Late Prehistory as evidenced by new bioarchaeological data from the Caucasus. *Sci. Rep.* **11**, 13124 (2021).
6. Sneha, M. L. & Arjun, R. Medicinal knowledge In South India (during neolithic to early historic period): an analysis of staple plant dietary nutrition. *CMDR J. Soc. Res.* **1**, 35–48 (2024).
7. Lightfoot, E., Liu, X. & Jones, M. K. Why move starchy cereals? A review of the isotopic evidence for prehistoric millet consumption across Eurasia. *World Archaeol.* **45**, 574–623 (2013).
8. Drucker, D. G. The isotopic ecology of the mammoth steppe. *Annu. Rev. Earth Planet. Sci.* **50**, 395–418 (2022).
9. Drucker, D. G. et al. Ecology of large ungulates in the northeastern Iberian Peninsula during the Upper Palaeolithic through stable isotopes and tooth wear analysis. *Quat. Environ. Hum.* **2**, 100011 (2024).
10. Terry, R. C., Guerre, M. E. & Taylor, D. S. How specialized is a diet specialist? Niche flexibility and local persistence through time of the Chisel-toothed kangaroo rat. *Funct. Ecol.* **31**, 1921–1932 (2017).
11. Saarinen, J., Mantzouka, D. & Sakala, J. Aridity, cooling, open vegetation, and the evolution of plants and animals during the cenozoic. In *Nature through Time*, edited by E. Martinetto, E. Tschopp & R. A. Gastaldo, pp. 83–107 (Springer International Publishing, Cham, 2020).
12. Prasifka, J. & Heinz, K. The use of C3 and C4 plants to study natural enemy movement and ecology, and its application to pest management. *Int. J. Pest Manag.* **50**, 177–181 (2004).
13. Cerling, T. E., Wang, Y. & Quade, J. Expansion of C4 ecosystems as an indicator of global ecological change in the late Miocene. *Nature* **361**, 344–345 (1993).
14. Farquhar, G. D. On the nature of carbon isotope discrimination in C4 species. *Funct. Plant Biol.* **10**, 205 (1983).
15. O'Leary, M. H. Carbon isotope fractionation in plants. *Phytochemistry* **20**, 553–567 (1981).
16. Ambrose, S. H. Isotopic Analysis of Paleodiets: Methodological and Interpretative Considerations. In *Investigations of ancient human tissue. Chemical analyses in anthropology*, edited by M. K. Sandford, pp. 59–130 (Gordon and Breach, Philadelphia, 1993).
17. Lee-Thorp, J. A. On isotopes and old bones. *Archaeometry* **50**, 925–950 (2008).
18. Kellner, C. M. & Schoeninger, M. J. A simple carbon isotope model for reconstructing prehistoric human diet. *Am. J. Phys. Anthropol.* **133**, 1112–1127 (2007).
19. Froehle, A. W., Kellner, C. M. & Schoeninger, M. J. Multivariate carbon and nitrogen stable isotope model for the reconstruction of prehistoric human diet. *Am. J. Phys. Anthropol.* **147**, 352–369 (2012).
20. van Klinken, G. J., Richards, M. P. & Hedges, R. E. M. An Overview of Causes for Stable Isotopic Variations in Past European Human Populations. Environmental, Ecophysiological, and Cultural Effects. In *Biogeochemical approaches to paleodietary analysis*. *Advances in archaeological and museum science*, edited by S. H. Ambrose & M. A. Katzenberg, pp. 39–63 (New York, London, 2002).
21. Cooper, C. G., Cooper, M. D., Richards, M. P. & Schmitt, J. Geographic and seasonal variation in δ13C values of C3 plant arabidopsis: Archaeological implications. *J. Archaeol. Sci.* **149**, 105709 (2023).
22. van Klinken, G. J., van der Plicht, J. & Hedges, R. E. M. Bone 13C/12C ratios reflect (palaeo) climatic variations. *Geophys. Res. Lett.* **21**, 445–448 (1994).
23. Hedges, R. E., Stevens, R. E. & Richards, M. Bone as a stable isotope archive for local climatic information. *Quat. Sci. Rev.* **23**, 959–965 (2004).
24. Lightfoot, E. et al. Carbon and nitrogen isotopic variability in foxtail millet (Setaria italica) with watering regime. *Rapid Commun. Mass Spectrom.* **34**, e8615 (2020).
25. An, C.-B. et al. Variability of the stable carbon isotope ratio in modern and archaeological millets: evidence from northern China. *J. Archaeol. Sci.* **53**, 316–322 (2015).
26. Dong, Y. et al. The potential of stable carbon and nitrogen isotope analysis of foxtail and broomcorn millets for investigating ancient farming systems. *Front. plant Sci.* **13**, 1018312 (2022).
27. Depaermentier, M. L. C. Isotopic dataset to: Depaermentier, MLC, Kempf, M, Motuzaitė Matuzevičiūtė, G. "Environmentally adjusted δ13C thresholds for accurate detection of C4 plant consumption in Europe" (2025).
28. Araus, J. L. et al. Identification of Ancient Irrigation Practices based on the Carbon Isotope Discrimination of Plant Seeds: a Case Study from the South-East Iberian Peninsula. *J. Archaeol. Sci.* **24**, 729–740 (1997).
29. Lightfoot, E. & Stevens, R. E. Stable isotope investigations of charred barley (Hordeum vulgare) and wheat (Triticum spelta) grains from Danebury Hillfort: implications for palaeodietary reconstructions. *J. Archaeol. Sci.* **39**, 656–662 (2012).
30. Gron, K. J. et al. Archaeological cereals as an isotope record of long-term soil health and anthropogenic amendment in southern Scandinavia. *Quat. Sci. Rev.* **253**, 106762 (2021).
31. Hald, M. M. et al. Farming during turbulent times: agriculture, food crops, and manuring practices in bronze age to viking age Denmark. *J. Archaeol. Sci. Rep.* **58**, 104736 (2024).
32. Nitsch, E. et al. A bottom-up view of food surplus: using stable carbon and nitrogen isotope analysis to investigate agricultural strategies and diet at Bronze Age Archontiko and Thessaloniki Toumba, northern Greece. *World Archaeol.* **49**, 105–137 (2017).
33. Heaton, T. H., Jones, G., Halstead, P. & Tsipropoulos, T. Variations in the 13C/12C ratios of modern wheat grain, and implications for interpreting data from Bronze Age Assiros Toumba, Greece. *J. Archaeol. Sci.* **36**, 2224–2233 (2009).
34. Aguilera, M., Zech-Matterne, V., Lepetz, S. & Balasse, M. Crop fertility conditions in north-eastern Gaul during the la tène and roman periods: a combined stable isotope analysis of archaeobotanical and archaeozoological remains. *Environ. Archaeol.* **23**, 323–337 (2018).
35. Alagich, R., Gardeisen, A., Alonso, N., Rovira, N. & Bogaard, A. Using stable isotopes and functional weed ecology to explore social differences in early urban contexts: the case of Lattara in mediterranean France. *J. Archaeol. Sci.* **93**, 135–149 (2018).
36. Antanaitis, I. & Ogrinc, N. Chemical analysis of bone: stable isotope evidence of the diet of Neolithic and Bronze Age people In Lithuania. *Istorija* **XLV**, 3–12 (2000).
37. Araus, J. L. & Buxó, R. Changes in carbon isotope discrimination in grain cereals from the north-western mediterranean basin during the past seven millenia. *Funct. Plant Biol.* **20**, 117 (1993).
38. Araus, J. L. et al. Changes in carbon isotope discrimination in grain cereals from different regions of the western Mediterranean Basin during the past seven millennia. Palaeoenvironmental evidence of a

differential change in aridity during the late Holocene. *Glob. Change Biol.* **3**, 107–118 (1997).
39. Araus, J. L. et al. Isotope and morphometrical evidence reveals the technological package associated with agriculture adoption in western Europe. *PNAS* **121**, e2401065121 (2024).
40. Ben Makhad, S. et al. Crop manuring on the Beauce plateau (France) during the second iron age. *J. Archaeol. Sci.: Rep.* **43**, 103463 (2022).
41. Bernardini, S. et al. New multi-proxy isotopic data on the copper age of eastern Liguria. *Riv. di Sci. Preistoriche* **LXXIII S3**, 1037–1043 (2023).
42. Bogaard, A. et al. From traditional farming in morocco to early urban agroecology in northern mesopotamia: combining present-day arable weed surveys and crop isotope analysis to reconstruct past agrosystems in (semi-)arid regions. *Environ. Archaeol.* **23**, 303–322 (2018).
43. Bogaard, A. et al. Crop manuring and intensive land management by Europe's first farmers. *Proc. Natl. Acad. Sci. USA* **110**, 12589–12594 (2013).
44. Cortese, F. et al. *Isotopic reconstruction of the subsistence strategy for a Central Italian Bronze Age community (Pastena cave, 2 nd millennium BCE)* (2022).
45. DiBenedetto, K. E. *Investigating Land Use by the Inhabitants of Western Cyprus During the Early Neolithic* (2018).
46. Eklund, M. *Changing Agriculture. Stable isotope analysis of charred cereals from Iron Age Öland*. (Master thesis, Stockholm University, Stockholm, 2019).
47. Fernández-Crespo, T., Ordoño, J., Bogaard, A., Llanos, A. & Schulting, R. A snapshot of subsistence in Iron Age Iberia: the case of La Hoya village. *J. Archaeol. Sci.: Rep.* **28**, 102037 (2019).
48. Fiorentino, G. et al. Third millennium B.C. climate change in Syria highlighted by Carbon stable isotope analysis of 14C-AMS dated plant remains from Ebla. *Palaeogeogr. Palaeoclimatol. Palaeoecol.* **266**, 51–58 (2008).
49. Fiorentino, G., Caracuta, V., Casiello, G., Longobardi, F. & Sacco, A. Studying ancient crop provenance: implications from δ(13)C and δ(15)N values of charred barley in a Middle Bronze Age silo at Ebla(NW Syria). *Rapid Commun. Mass Spectrom.* **26**, 327–335 (2012).
50. García-Collado, M. I. et al. First direct evidence of agrarian practices in the alava plateau (northern liberia) during the middle ages through carbon and nitrogen stable isotope analyses of charred seeds. *Environ. Archaeol.* 1–11 (2022).
51. Gavériaux, F. et al. L'alimentation des premières sociétés agropastorales du Sud de la France: premières données isotopiques sur des graines et fruits carbonisés néolithiques et essais de modélisation. *Comptes Rendus. Palevol*. (2021).
52. Gavériaux, F., Motta, L., Bailey, P., Brilli, M. & Sadori, L. Crop husbandry at gabii during the iron age and archaic period: the archaeobotanical and stable isotope evidence. *Environ. Archaeol.* **29**, 370–383 (2024).
53. Gillis, R. E. et al. Stable isotopic insights into crop cultivation, animal husbandry, and land use at the Linearbandkeramik site of Vráble-Veľké Lehemby (Slovakia). *Archaeol. Anthropol. Sci.* **12**; https://doi.org/10.1007/s12520-020-01210-2 (2020).
54. Gron, K. J. et al. Nitrogen isotope evidence for manuring of early Neolithic Funnel Beaker Culture cereals from Stensborg, Sweden. *J. Archaeol. Sci.: Rep.* **14**, 575–579 (2017).
55. Halvorsen, L. S., Mørkved, P. T. & Hjelle, K. L. Were prehistoric cereal fields in western Norway manured? Evidence from stable isotope values (δ15N) of charred modern and fossil cereals. *Veget. Hist. Archaeobot.* **32**, 583–596 (2023).
56. Fraser, R. A., Bogaard, A., Schäfer, M., Arbogast, R. & Heaton, T. H. E. Integrating botanical, faunal and human stable carbon and nitrogen isotope values to reconstruct land use and palaeodiet at LBK Vaihingen an der Enz, Baden-Württemberg. *World Archaeol.* **45**, 492–517 (2013).
57. Isaakidou, V. et al. Changing land use and political economy at neolithic and bronze Age Knossos, Crete: stable carbon (δ 13 C) and nitrogen (δ 15 N) isotope analysis of charred crop grains and faunal bone collagen. *Proc. Prehist. Soc.* **88**, 155–191 (2022).
58. Kanstrup, M. *When δ15N values reveal manuring practice. Empirical evidence from fieldwork, charring experiments and archaeobotanical remains* (Aarhus Universitet, Institut for Agroøkologi, Aarhus, 2012).
59. Karakaya, D. Botanical Aspects of the Environment and Economy at Tell Tayinat from the Bronze to Iron Ages (ca. 2.200–600 BCE), In *south-central Turkey* (Doctoral Dissertation, Universität Tübingen (Germany), Doctoral Dissertation, Universität Tübingen (Germany, 2020).
60. Karaliūtė, R., Motuzaitė Matuzevičiūtė, G., Styring, A. & Stroud, E. 2600 Years of farming in Eastern Lithuania: soil management according to ancient barley isotopic values. *Quaternary Environments and Humans* (in preparation).
61. Knipper, C. et al. What is on the menu in a Celtic town? Iron age diet reconstructed at Basel-Gasfabrik, Switzerland. *Archaeol. Anthropol. Sci.* **9**, 1307–1326 (2017).
62. Knipper, C. et al. Reconstructing Bronze Age diets and farming strategies at the early Bronze Age sites of La Bastida and Gatas (southeast Iberia) using stable isotope analysis. *PloS One* **15**, e0229398 (2020).
63. Lodwick, L. Cultivating villa economies: archaeobotanical and isotopic evidence for iron age to roman agricultural practices on the chalk downlands of Southern Britain. *Eur. j. archaeol.* **26**, 445–466 (2023).
64. Lodwick, L., Campbell, G., Crosby, V. & Müldner, G. Isotopic evidence for changes in cereal production strategies in iron age and Roman Britain. *Environ. Archaeol.* **26**, 13–28 (2021).
65. Maltas, T., Şahoğlu, V., Erkanal, H. & Tuncel, R. From horticulture to agriculture: New data on farming practices in Late Chalcolithic western Anatolia. *J. Archaeol. Sci.: Rep.* **43**, 103482 (2022).
66. Martínez Sánchez, R. M. et al. Archaeology, chronology, and age-diet insights of two late fourth millennium cal BC pit graves from central southern Iberia (Córdoba, Spain). *Int. J. Osteoarchaeol.* **30**, 245–255 (2020).
67. Messager, E. et al. Archaeobotanical and isotopic evidence of Early Bronze Age farming activities and diet in the mountainous environment of the South Caucasus: a pilot study of Chobareti site (Samtskhe–Javakheti region). *J. Archaeol. Sci.* **53**, 214–226 (2015).
68. Minkevičius, K. et al. New insights into the subsistence economy of the Late Bronze Age (1100–400 cal BC) communities in the southeastern Baltic. *Archaeol. Balt.* **30**, 58–79 (2023).
69. Mnich, B. et al. Terrestrial diet in prehistoric human groups from southern Poland based on human, faunal and botanical stable isotope evidence. *J. Archaeol. Sci.: Rep.* **32**, 102382 (2020).
70. Mora-González, A. et al. The isotopic footprint of irrigation in the western Mediterranean basin during the Bronze Age: the settlement of Terlinques, southeast Iberian Peninsula. *Veget Hist. Archaeobot.* **25**, 459–468 (2016).
71. Mora-González, A., Teira-Brión, A., Granados-Torres, A., Contreras-Cortés, F. & Delgado-Huertas, A. Agricultural production in the 1st millennium BCE in Northwest Iberia: results of carbon isotope analysis. *Archaeol. Anthropol. Sci.* **11**, 2897–2909 (2019).
72. Mueller-Bieniek, A. et al. Spatial and temporal patterns in Neolithic and Bronze Age agriculture in Poland based on the stable carbon and nitrogen isotopic composition of cereal grains. *J. Archaeol. Sci.: Rep.* **27**, 101993 (2019).

73. Niekamp, A. N. *Crop growing conditions and agricultural practices in bronze age greece: a stable isotope analysis of archaeobotanical remains from Tsoungiza* (Master's thesis, University of Cincinnati, 2016).
74. Nitsch, E. K., Jones, G., Sarpaki, A., Hald, M. M. & Bogaard, A. Farming practice and land management at Knossos, Crete: new insights from δ13C and δ15N analysis of Neolithic and Bronze Age crop remains. In *Country in the City: Agricultural functions of protohistoric urban settlements (Aegean and Western Mediterranean)*, edited by D. Garcia, R. Orgeolet, M. Pomadère & J. Zurbach (Archaeopress, Oxford, 2019), pp. 159–173.
75. O'connell, T. C. et al. Living and dying at the Portus Romae. *Antiquity* **93**, 719–734 (2019).
76. Pate, F. D., Henneberg, R. J. & Henneberg, M. Stable carbon and nitrogen isotope evidence for dietary variability at ancient Pompeii, Italy; https://doi.org/10.5281/zenodo.35526 (2015).
77. Pilaar Birch, S. E. et al. Herd management and subsistence practices as inferred from isotopic analysis of animals and plants at Bronze Age Politiko-Troullia, Cyprus. *PloS One* **17**, e0275757 (2022).
78. Piličiauskas, G. et al. The earliest evidence for crop cultivation during the Early Bronze Age in the southeastern Baltic. *J. Archaeol. Sci.: Rep.* **36**, 102881 (2021).
79. Riehl, S., Bryson, R. & Pustovoytov, K. Changing growing conditions for crops during the Near Eastern Bronze Age (3000–1200 BC): the stable carbon isotope evidence. *J. Archaeol. Sci.* **35**, 1011–1022 (2008).
80. Speciale, C. et al. The case study of Case Bastione: first analyses of 3rd millennium cal BC paleoenvironmental and subsistence systems in central Sicily. *J. Archaeol. Sci.: Rep.* **31**, 102332 (2020).
81. Styring, A. K. et al. Urban form and scale shaped the agroecology of early 'cities' in northern Mesopotamia, the Aegean and Central Europe. *J. Agrar. Change* **22**, 831–854 (2022).
82. Vaiglova, P. et al. An integrated stable isotope study of plants and animals from Kouphovouno, southern Greece: a new look at Neolithic farming. *J. Archaeol. Sci.* **42**, 201–215 (2014).
83. Vaiglova, P. et al. Of cattle and feasts: Multi-isotope investigation of animal husbandry and communal feasting at Neolithic Makriyalos, northern Greece. *PloS One* **13**, e0194474 (2018).
84. Vaiglova, P. et al. Exploring diversity in neolithic agropastoral management in mainland greece using stable isotope analysis. *Environ. Archaeol.* **28**, 62–85 (2021).
85. Vanhanen, S. & Ilves, K. Flax use, weeds and manuring in Viking Age Åland: archaeobotanical and stable isotope analysis. *Veget. Hist. Archaeobot.* **34**, 501–517 (2025).
86. Varalli, A. et al. Bronze Age innovations and impact on human diet: a multi-isotopic and multi-proxy study of western Switzerland. *PloS One* **16**, e0245726 (2021).
87. Varalli, A. et al. Insights into the frontier zone of Upper Seine Valley (France) during the Bronze Age through subsistence strategies and dietary patterns. *Archaeol. Anthropol. Sci.* **15**; https://doi.org/10.1007/s12520-023-01721-8 (2023).
88. Wallace, M. P. et al. Stable carbon isotope evidence for neolithic and bronze age crop water management in the Eastern Mediterranean and Southwest Asia. *PloS One* **10**, e0127085 (2015).
89. Lempiäinen-Avci, M. et al. New insight into medieval cultivation at the village of Mankby in Espoo, Finland – comparing stable isotopes of carbon $\delta^{13}C$ and nitrogen $\delta^{15}N$ of Secale and Hordeum from Mankby to 14th century grain materials from Estonia. In *Shattered and Scattered Pasts. Festschrift for Professor Georg Haggrén*, edited by T. Heinonen, et al., pp. 68–85 (Waasa Graphics, Vaasa, 2025).
90. Ferrio, J. P., Alonso, N., Voltas, J. & Araus, J. L. Grain weight changes over time in ancient cereal crops: Potential roles of climate and genetic improvement. *J. Cereal Sci.* **44**, 323–332 (2006).
91. Della Penna, V. *Tradizione e modernità delle pratiche agricole nei Monti dauni: storia e archeologia dei sistemi agroalimentari subappenninici* (Unpublished dissertation, Università degli Studi di Foggia, 2022).
92. Dreslerová, D. et al. Maintaining soil productivity as the key factor in European prehistoric and Medieval farming. *J. Archaeol. Sci.: Rep.* **35**, 102633 (2021).
93. Drtikolová Kaupová, S. et al. Stav izotopových výzkumů stravy, rezidenční mobility a zemědělského hospodaření populace Velké Moravy (9.–10. století). *Arch. Rozhl.* **74**, 203–240 (2022).
94. Hamerow, H. et al. An integrated bioarchaeological approach to the medieval 'agricultural revolution': a case study from Stafford, England, c.ad 800–1200. *Eur. j. archaeol.* **23**, 585–609 (2020).
95. Herrscher, E. et al. Dietary practices, cultural and social identity in the Early Bronze Age southern Caucasus. *Paléorient*, 151–174; (2021).
96. Látková, M., Skála, R. & Drtikolová Kaupová, S. Bioarchaeological characteristics of the wheat (triticum aestivum) consumed at different parts of the early medieval settlement agglomeration of Mikulčice-Kopčany (9th–10th Century AD, Czech Republic). *Environ. Archaeol.* **30**, 267–279 (2025).
97. Reed, K. & Wallace, M. To pretreat, or not to pretreat, that is the question. The value of pretreatment protocols in the stable carbon and nitrogen isotope analysis of archaeobotanical cereal grains from Croatia and Serbia. *Sci. Technol. Archaeol. Res.* **10**; https://doi.org/10.1080/20548923.2024.2410092 (2024).
98. Russell, N., Cook, G. T., Ascough, P., Barrett, J. H. & Dugmore, A. Species specific marine radiocarbon reservoir effect: a comparison of ΔR values between Patella vulgata (limpet) shell carbonate and Gadus morhua (Atlantic cod) bone collagen. *J. Archaeol. Sci.* **38**, 1008–1015 (2011).
99. Schlütz, F. et al. Stable isotope analyses (δ15N, δ34S, δ13C) locate early rye cultivation in northern Europe within diverse manuring practices. *Philos. Trans. R. Soc. Lond. Ser. B, Biol. Sci.* **380**, 20240195 (2025).
100. Treasure, E. R. The frontier of Islam: an archaeobotanical study of agriculture in the Iberian Peninsula (c.700 – 1500 CE) (Unpublished dissertation, Durham University, 2020).
101. Vaiglova, P. *Neolithic agricultural management in the Eastern Mediterranean: new insight from a multi-isotope approach* (Doctoral dissertation, University of Oxford, 2016).
102. Olson, D. M. et al. Terrestrial ecoregions of the world: a new map of life on earth. *BioScience* **51**, 933 (2001).
103. Larsson, M., Bergman, J. & Olsson, P. A. Soil, fertilizer and plant density: Exploring the influence of environmental factors to stable nitrogen and carbon isotope composition in cereal grain. *J. Archaeol. Sci.* **163**, 105935 (2024).
104. Filipović, D. et al. New AMS 14C dates track the arrival and spread of broomcorn millet cultivation and agricultural change in prehistoric Europe. *Sci. Rep.* **10**, 13698 (2020).
105. Vaiglova, P., Lazar, N. A., Stroud, E. A., Loftus, E. & Makarewicz, C. A. Best practices for selecting samples, analyzing data, and publishing results in isotope archaeology. *Quat. Int.*; https://doi.org/10.1016/j.quaint.2022.02.027 (2023).
106. Hedges, R. E. M. Isotopes and red herrings: comments on Milner et al. and Lidén et al. *Antiquity* **78**, 34–37 (2004).
107. O'Regan, H. J., Lamb, A. L. & Wilkinson, D. M. The missing mushrooms: Searching for fungi in ancient human dietary analysis. *J. Archaeol. Sci.* **75**, 139–143 (2016).
108. Drucker, D. G., Bridault, A., Hobson, K. A., Szuma, E. & Bocherens, H. Can carbon-13 in large herbivores reflect the canopy effect in temperate and boreal ecosystems? Evidence from modern and ancient ungulates. *Palaeogeogr. Palaeoclimatol. Palaeoecol.* **266**, 69–82 (2008).

109. Bonafini, M., Pellegrini, M., Ditchfield, P. & Pollard, A. M. Investigation of the 'canopy effect' in the isotope ecology of temperate woodlands. *J. Archaeol. Sci.* **40**, 3926–3935 (2013).
110. Häberle, S. et al. Carbon and nitrogen isotopic ratios in archaeological and modern Swiss fish as possible markers for diachronic anthropogenic activity in freshwater ecosystems. *J. Archaeol. Sci.: Rep.* **10**, 411–423 (2016).
111. Guiry, E. Complexities of stable carbon and nitrogen isotope biogeochemistry in ancient freshwater ecosystems: implications for the study of past subsistence and environmental change. *Front. Ecol. Evol*. **7**; https://doi.org/10.3389/fevo.2019.00313 (2019).
112. Robson, H. K. et al. Carbon and nitrogen stable isotope values in freshwater, brackish and marine fish bone collagen from Mesolithic and Neolithic sites in central and northern Europe. *Environ. Archaeol.* **21**, 105–118 (2016).
113. Göhring, A., Hölzl, S., Mayr, C. & Strauss, H. Identification and quantification of the sea spray effect on isotopic systems in α-cellulose (δ13C, δ18O), total sulfur (δ34S), and 87Sr/86Sr of European beach grass (Ammophila arenaria, L.) in a greenhouse experiment. *Sci. Total Environ.* **856**, 158840 (2023).
114. Büntgen, U. Scrutinizing tree-ring parameters for Holocene climate reconstructions. *WIREs Clim. Change* **13**; https://doi.org/10.1002/wcc.778 (2022).
115. Montgomery, J. et al. Strategic and sporadic marine consumption at the onset of the Neolithic: increasing temporal resolution in the isotope evidence. *Antiquity* **87**, 1060–1072 (2013).
116. Göhring, A., Hölzl, S., Mayr, C. & Strauss, H. Multi-isotope fingerprints of recent environmental samples from the Baltic coast and their implications for bioarchaeological studies. *Sci. Total Environ.* **874**, 162513 (2023).
117. Hopkins, J. B. & Ferguson, J. M. Correction: estimating the diets of animals using stable isotopes and a comprehensive bayesian mixing model. *PloS One* **7**; https://doi.org/10.1371/annotation/d222580b-4f36-4403-bb1f-cfd449a5ed74 (2012).
118. Ferrio, J. P., Araus, J. L., Buxó, R., Voltas, J. & Bort, J. Water management practices and climate in ancient agriculture: inferences from the stable isotope composition of archaeobotanical remains. *Veget. Hist. Archaeobot.* **14**, 510–517 (2005).
119. Jones, P. J., O'Connell, T. C., Jones, M. K., Singh, R. N. & Petrie, C. A. Crop water status from plant stable carbon isotope values: a test case for monsoonal climates. *Holocene* **31**, 993–1004 (2021).
120. Szpak, P., Metcalfe, J. Z. & Macdonald, R. A. Best practices for calibrating and reporting stable isotope measurements in archaeology. *J. Archaeol. Sci.: Rep.* **13**, 609–616 (2017).
121. Salesse, K. et al. IsoArcH.eu: an open-access and collaborative isotope database for bioarchaeological samples from the Graeco-Roman world and its margins. *J. Archaeol. Sci.: Rep.* **19**, 1050–1055 (2018).
122. Farese, M. MAIA: mediterranean archive of isotopic dAta. *Pandora* https://doi.org/10.48493/55v1-xg54 (2023).
123. Formichella, G., Soncin, S. & Cocozza, C. Isotòpia: a stable isotope database for classical antiquity. *Pandora* **v.1 19.09.2023**; https://doi.org/10.48493/m0m0-b436 (2023).
124. Mantile, N., Fernandes, R., Lubritto, C. & Cocozza, C. IsoMedIta: a stable isotope database for Medieval Italy. *Res. Data J. Humanit. Soc. Sci.* **8**, 1–13 (2023).
125. Cocozza, C., Cirelli, E., Groß, M., Teegen, W.-R. & Fernandes, R. Presenting the compendium isotoporum medii aevi, a multi-isotope database for Medieval Europe. *Sci. Data* **9**, 354 (2022).
126. Graven, H., Keeling, R. F. & Rogelj, J. Changes to carbon isotopes in atmospheric CO2 over the industrial era and into the future. *Glob. Biogeochem. Cycles* **34**, e2019GB006170 (2020).
127. Nitsch, E. K., Charles, M. & Bogaard, A. Calculating a statistically robust δ 13 C and δ 15 N offset for charred cereal and pulse seeds. *Sci. Technol. Archaeol. Res.* **1**, 1–8 (2015).
128. Stroud, E., Charles, M., Bogaard, A. & Hamerow, H. Turning up the heat: Assessing the impact of charring regime on the morphology and stable isotopic values of cereal grains. *J. Archaeol. Sci.* **153**, 105754 (2023).
129. Teira-Brión, A., Stroud, E., Charles, M. & Bogaard, A. The effects of charring on morphology and stable carbon and nitrogen isotope values of common and foxtail millet grains. *Front. Environ. Archaeol*. **3**; https://doi.org/10.3389/fearc.2024.1473593 (2024).
130. Varalli, A., D'Agostini, F., Madella, M., Fiorentino, G. & Lancelotti, C. Charring effects on stable carbon and nitrogen isotope values on C4 plants: Inferences for archaeological investigations. *J. Archaeol. Sci.* **156**, 105821 (2023).
131. Styring, A. K. et al. Recommendations for stable isotope analysis of charred archaeological crop remains. *Front. Environ. Archaeol.* **3**; https://doi.org/10.3389/fearc.2024.1470375 (2024).
132. R. Core Team. *R: A language and environment for statistical* (R Foundation for Statistical Computing, Vienna, 2021).
133. Bates, D., Mächler, M., Bolker, B. & Walker, S. Fitting linear mixed-effects models using lme4. *J. Stat. Soft*. **67**; https://doi.org/10.18637/jss.v067.i01 (2015).
134. Hijmans, R. J. *_terra: Spatial Data Analysis_* (2024).
135. Pebesma, E. & Bivand, R. *Spatial Data Science* (Chapman and Hall/CRC, New York, 2023).
136. Pebesma, E. Simple Features for R: standardized support for spatial vector data. *R. J.* **10**, 439 (2018).
137. Warnes, G. et al. *_gtools: Various R Programming Tools_* (2023).
138. Wickham, H., François, R., Henry, L., Müller, K. & Vaughan, D. *_dplyr: A Grammar of Data Manipulation_* (2023).
139. Wickham, H. *Ggplot2. Elegant graphics for data analysis* (Springer Science+Business Media, LLC, New York, NY, 2016).
140. Dunnington, D. *_ggspatial: Spatial Data Framework for ggplot2_* (2023).
141. Auguie, B. *_gridExtra: Miscellaneous Functions for "Grid" Graphics* (2017).
142. Kempf, M. Environmental data to: Depaermentier, MLC; Kempf, M; Motuzaitė Matuzevičiūtė, G: environmentally adjusted δ13C thresholds for accurate detection of C4 plant consumption in Europe (2025).
143. Karger, D. N. et al. Climatologies at high resolution for the earth's land surface areas. *Sci. Data* **4**, 170122 (2017).
144. South, A., Michael, S. & Massicotte, P. *rnaturalearthdata: world vector map data from natural earth used in 'rnaturalearth'* (2017).

Acknowledgements

M.L.C.D. and G.M.M. were funded by the European Union with a Consolidator Grant awarded to Giedrė Motuzaitė Matuzevičiūtė (ERC-CoG, MILWAYS, 101087964). Views and opinions expressed are those of the authors only and do not necessarily reflect those of the European Union or the European Research Council Executive Agency. Neither the European Union nor the granting authority can be held responsible for them. MK's research is funded by the Swiss National Science Foundation (SNSF/SNF): Project EXOCHAINS – Exploring Holocene Climate Change and Human Innovations across Eurasia (SNSF grant number: TMPFP2_217358).

Author contributions

Conceptualization: M.L.C.D., M.K. and G.M.M. Isotope data collection and formal analyses: M.L.C.D. Environmental and cluster analyses: M.K. Writing: M.L.C.D and M.K. Editing: M.L.C.D., M.K., G.M.M. Visualisation: M.K. and M.L.C.D. Revision: M.L.C.D., M.K.

Competing interests

The authors declare no competing interests.

Additional information

Supplementary information The online version contains supplementary material available at https://doi.org/10.1038/s43247-025-03031-4.

Correspondence and requests for materials should be addressed to Margaux L. C. Depaermentier or Michael Kempf.

Peer review information *Communications Earth & Environment* thanks Ashley McCall and the other, anonymous, reviewer(s) for their contribution to the peer review of this work. Primary Handling Editors: Nicola Colombo and Aliénor Lavergne. [A peer review file is available].